



universität  
wien

# Diplomarbeit

Titel der Diplomarbeit:

## **3D Geometric Morphometric Analysis of the Maxillary 2<sup>nd</sup> Molar in Cave Bears (*sensu lato*)**

verfasst von:

**Eric John Mazelis**

angestrebter akademischer Grad:

Magister der Naturwissenschaften (Mag. rer. nat.)

Wien, 2013

Studienkennzahl lt. Studienblatt:  
Studienrichtung lt. Studienblatt:

A057-437  
Individuelles Diplomstudium Quartärbiologie und  
Archäologie des Paleolithikum  
Univ. Prof. Dr. *Gerhard W. Weber*

Betreut von:

# **3D Geometric Morphometric Analysis of the Maxillary 2<sup>nd</sup> Molar in Cave Bears (*sensu lato*)**

# A) Index

Chapter	Chapter title	Subchapter	Sub-Subchapter	Pages
A	Index			3
B	List of abbreviations			4
1	Introduction			4
2	Material and Methods			6
2.1		Sites		6
2.1.1			Schwabenreithöhle, Austria	7
2.1.2			Ander dles Conturines, Italy	7
2.1.3			Gamssulzenhöhle, Austria	7
2.1.4			Elevation above Mean Sea Level	8
2.1.5			Dating	8
2.2		Species		10
2.2.1			<i>Ursus eremus</i>	11
2.2.2			<i>Ursus ladinicus</i>	12
2.2.3			<i>Ursus ingressus</i>	12
2.2.4			Genetic Analysis	13
2.2.5			Body Size	13
2.3		Element and Sample		14
2.3.1			Length of tooth row p4 – m3	16
2.4		3D Models and Programs		17
2.4.1			CT scanner (Vienna Micro-CT Lab)	17
2.4.2			AMIRA (VSG – Visualization Science Group, France)	17
2.4.3			EVAN Toolbox (EVAN-Society e.V.)	18
2.4.4			Morphologika2 (v.2.5)	18
2.5		Landmarks		19
2.6		Generalized Procrustes Analysis (GPA) and Principal Components Analysis (PCA)		22
2.7		Regression of PC Scores on Centroid Size		23
2.7.1			Centroid Size	23
2.7.2			Allometry	23
2.8		Canonical Variance Analysis (CVA)		24
3	Results			24
3.1		Centroid Size		24
3.2		M <sup>2</sup> /Post-canine tooth row ratio		26
3.3		PCA in Shape Space		27
3.4		PCA in Form Space		38
3.5		Allometry		40
3.6		MANOVA/CVA		41
4	Discussion			42
5	Conclusion			44
6	Outlook			45
7	Acknowledgements			45
8	References			46
9	Abstract			50
10	Zusammenfassung			50
11	Appendix			52
12	Curriculum Vitae			54

Table 1 Index.

## B) List of Abbreviations

Abbreviation	Description	Abbreviation	Description
CU	Conturines cave	CT	Computed tomography
GS	Gamssulzen cave	ET	EVAN Toolbox
SW	Schwabenreith cave	Pa	Paracone
ID	Katasternumber	Me	Metacone
Cal. BP	Years Before Present (calibrated)	Pr	Protocone
C	Carbon	Hy	Hypocone
N	Nitrogen	Hys	Hypostyle
P	Maxillary premolar	GPA	Generalized Procrustes Analysis
p	Mandibular premolar	PCA	Principal Components Analysis
i	Mandibular incisor	PC	Principal Components
M	Maxillary molar	CS	Centroid Size
m	Mandibular molar	MANOVA	Multivariate Analysis of Variance
AMSL	Elevation Above Mean Sea Level	Sin	Sinistro (left)
U/Th	Uranium – Thorium	Dex	Dexter (right)
<i>et al.</i>	Et alia – And others	CVA	Canonical Variance Analysis
Mc	Metacarpal	mtDNA	Mitochondrial DNA
Mt	Metatarsal	bp	Base pairs

Table 2 List of abbreviations.

## 1) Introduction

Cave bears were the first members of the European megafauna to become extinct in the late Quaternary. Radiocarbon dating shows that their extinction (27,800 before present (BP)) coincides with the onset of the last glacial maximum in Europe, the Greenland Stadial 3 (27,500 BP) (Pacher & Stuart, 2008). Subsequent loss of suitable caves for hibernation, added predation pressure by humans and/or other predators such as lions (*Panthera leo spelaea*) or

hyena (*Crocuta crocuta spelaea*) (Nagel, 2000) and/or loss of suitable foods might have led to their extinction.

Based on analyses of stable isotopes  $^{13}\text{C}$  and  $^{15}\text{N}$ , Cave bears were most likely strict herbivores (e.g. Kurtén, 1976; Bocherens *et al.*, 1997; Vila Taboada *et al.*, 2001; Pacher & Stuart, 2008; Bocherens *et al.*, 2011; Pérez-Rama *et al.*, 2011; Bocherens *et al.*, 2013) with a mean body mass of 1,100 kg and the largest individuals weighing up to 1,500 kg (Rabeder *et al.*, 2000). The abundance of herbaceous pollen in fossil bearing cave deposits and the fact that a diet of tough high-alpine grasses would not be sustainable by the brachydont cave bear molars suggests that their diet consisted of herbaceous vegetation and possibly tubers (Hille & Rabeder, 1986; Döppes *et al.*, 2011).

The Pleistocene was a time of rapid climatic fluctuation (Fernández-Mosquera *et al.*, 2001) with likely corresponding changes in vegetation. Cave bears show highly variable teeth, meaning both, a high intraspecific variability as well as a great morphological overlap between species. It is likely that this high variability allowed cave bears (*sensu lato*) to survive changes in climate and adapt to different habitats.

This study will use the quantitative method of Virtual Anthropology (Weber and Bookstein 2011) and 3D geometric morphometrics to study different shapes in cave bear upper 2<sup>nd</sup> molars. While a qualitative analysis of single isolated teeth is mostly not sufficient for species identification (personal communication G. Rabeder), this quantitative analysis will take into account the overall shape and form of the tooth based on both the enamel surface and the underlying dentin structure with the goal to differentiate teeth on a species level.

The study uses shape and form differences of the upper 2<sup>nd</sup> molar within and between three species of cave bears (*Ursus eremus*, *U. ladinicus* and *U. ingressus*). The high intraspecific variability of cave bear upper 2<sup>nd</sup> molars may overshadow trends in shape and form among the studied taxa, which will be made visible with this approach.

A previous study of this element in *Ursus spelaeus* and *U. ingressus* by Seetah *et al.* (2012) demonstrated differences in shape in relation to geographic location. This indicates slight differences in diet, which could reflect climatic changes during the European late Pleistocene.

Although the median divergence date of the most recent common ancestor for all cave bears has been calculated, based on mtDNA analyses, to have lived some 660,000 years ago (Hofreiter *et al.*, 2002), the oldest dated cave bear remains are approximately 130,000 years old (Rabeder & Hofreiter, 2004). The rapid evolution and specialization on different diets (Bocherens *et al.*, 2011) and habitats among the three species are remarkable. The dentition of cave bears is highly variable (Rabeder, 1999; Rabeder *et al.*, 2000), which was certainly fundamental to their fast dental evolution, and is especially visible in the upper and lower P4 and the maxillary 2<sup>nd</sup> molar (M<sup>2</sup>).

The goals of this study are twofold: Establishing a landmark set that would allow classifying small samples of teeth into one of the three species and identifying differences in shape and form among the species, if possible.

## 2) Material and Methods

### 2.1) Sites

Each species will be represented by a separate European site, located at different elevations and representing different habitats. Species attribution in this sample is based on the fact that each of these sites was only occupied by a single cave bear species for the dated timeframes (Rabeder *et al.*, 2004).

The geographic coordinates in Table 3 were published by Döppes & Rabeder (eds., 1997) and Pacher & Stuart (2008). Gamssulzen cave and Schwabenreith cave are located approximately 60 kilometers apart from one another in linear distance. Conturines cave is located 200 kilometers further southwest of Gamssulzen cave.

Site	° Latitude	° Longitude
Gamssulzen cave	47° 40' 56"	14° 17' 52"
Schwabenreith cave	47° 50' 33"	14° 58' 38"
Conturines cave	46° 65'	12° 13'

Table 3 Geographic coordinates for the cave sites.

These caves have previously been discussed at length: A monograph on Gamssulzen cave was edited by Rabeder (1995) and several studies have been published on both the Conturines (e.g. Rabeder *et al.*, 1994; Rabeder *et al.*, 2006a) and Schwabenreith caves (e.g. Fladerer, 1992; Pacher, 2000). Specimens from all three caves have been included in many studies that focused on cave bear diet, morphology and evolution.

### **2.1.1 Schwabenreithhöhle, Austria**

Schwabenreith cave (ID: 1823/32) is located on the northern flank of the “Schöpfertaler Waldberg” near Lunz am See, Lower Austria. The entrance to the cave is located at 959 m above sea level. The cave was first explored in 1969, and several episodes of excavations started in the early 1970s (Fladerer, 1992). Due to their old geological age the specimens from this cave could not be dated using  $^{14}\text{C}$  radiocarbon dating. No bones were dated directly, but rather the sinter layers above (78,400 cal. BP) and below (116,000 cal. BP) the fossil-rich soil layer were both dated using the Uranium-Thorium dating method.

### **2.1.2 Ander dles Conturines, Italy**

Conturines cave is situated at 2,775 m above sea level on Conturines Mountain in the Gadertaler Dolomite Mountain range, Italy. Numerous excavations have been carried out between the late 1980s and early 2000s (Rabeder *et al.*, 2006a). Currently only one radiocarbon date exists for cave bear remains: 47,685 cal. BP (Pacher & Stuart, 2008). Other fossil ages fell outside the range of radiocarbon dating and dates were collected by Uranium-Thorium dating, ranging between 115,800 and 41,900 BP, indicating occupation during the Würm glacial period (Rabeder *et al.*, 1994).

### **2.1.3 Gamssulzenhöhle, Austria**

Gamssulzen cave (ID: 1637/3) is located in the northwestern flank of the Seespitz Mountain in the Totes Gebirge mountain range in Austria. The entrance to the cave is located 1,300 m above sea level and is thus considered to be high-alpine. The cave was discovered and explored in the early 20<sup>th</sup> century. Excavations were conducted in the late 1980s and early 1990s (Rabeder, 1995). Cave bear fossils were dated to between 51,256 and 25,400 years cal. BP using  $^{14}\text{C}$  radiocarbon dating (Rabeder, 1995; Pacher & Stuart, 2008). The cave was used as a hibernation den by cave bears for at least 25,000 years during the Late Würmian glacial.

## 2.1.4 Elevation above Mean Sea Level

The elevation above current mean sea level in meters indicates the elevation of the current cave entrances (Table 4). The sea level during the Pleistocene was generally lower than it is today due to the Quaternary glaciation during which large amounts of water were trapped as permanent ice sheets on the poles and in glaciers. During the times of occupation for each of the caves the entrances of the caves could have been at slightly different elevations. While this may not necessarily be the ancient entrance that was used by the cave bears it will be used as an approximation of the elevation of the entire cave. In some caves the paths the bears took to navigate the caves can be reconstructed by following polished rock surfaces inside the caves, so called “Bärenschliff”, which are the result of bears walking close to the walls in the dark and smoothing the wall surfaces over time (Rosendahl & Döppes, 2006).

While it is known that cave bears hibernated in these caves (Rabeder, 1999; Germonpré & Sablin, 2001; Withalm, 2008; Peigne *et al.*, 2009; Pérez-Rama *et al.*, 2011), it was suggested that they may have also frequented them throughout the rest of the year (Döppes *et al.*, 2011) during bad weather or at night. This assumption is partially based on deciduous teeth, which were also found in the caves. Resorption on the roots indicates these teeth were lost naturally. In brown bears (*Ursus arctos*) the change of deciduous to permanent dentition normally happens during the months between May and September (Torres *et al.*, 2007). During the time of occupation we can assume that the vegetation line was located higher up on the mountains as the cave bears would not have wandered outside of a habitable environment.

Cave	Elevation (AMSL)
Schwabenreith cave	959 m
Gamssulzen cave	1,300 m
Conturines cave	2,775 m

Table 4 Elevation of cave entrances.

## 2.1.5 Dating

Table 5 lists all available radiometric dates (Radiocarbon  $^{14}\text{C}$  and Uranium-Thorium) directly or indirectly dating the sites in this study. The fossils in the Schwabenreith cave were not dated directly. The fossils from this site stem from a layer that was situated between two sinter layers. These were dated using Uranium-Thorium dating methods (Rabeder, 1999).



Direct radiocarbon dates exist for fossils from Gamssulzen cave and Conturines cave. Most specimens from Conturines have been dated using the Uranium-Thorium dating method due to the advanced geological age of the fossils (Rabeder *et al.*, 1994).

Since none of the specimens included in this study have been directly dated and the stratigraphy is disturbed, no relative or absolute dates can be assumed for the specimens, other than a minimum and maximum age.

Site	Dating Method	Calibrated Age in years	Error +/- (years)	Reference
Conturines	U/Th	18,100	+/- 400	Rabeder <i>et al.</i> , 1994
Conturines	U/Th	44,900	+/- 2,600	Rabeder <i>et al.</i> , 1994
Conturines	U/Th	> 336,000	-	Rabeder <i>et al.</i> , 1994
Conturines	U/Th	> 283,000	-	Rabeder <i>et al.</i> , 1994
Conturines	U/Th	108,200	+ 7,600 - 7,000	Rabeder <i>et al.</i> , 1994
Conturines	U/Th	69,000	+/- 2,600	Rabeder <i>et al.</i> , 1994
Conturines	U/Th	86,700	+ 4,700 - 4,600	Rabeder <i>et al.</i> , 1994
Conturines	<sup>14</sup> C	47,685	1,708	Hofreiter <i>et al.</i> , 2004
Schwabenreith	U/Th	78,400	+ 30,200 - 23,400	Rabeder & Withalm, 1995
Schwabenreith	U/Th	116,000	5,000	Rabeder & Withalm, 1995
Gamssulzen	U/Th	25,400	-	Rabeder 1995
Gamssulzen	<sup>14</sup> C	30,754	740	Rabeder 1995
Gamssulzen	<sup>14</sup> C	32,249	562	Rabeder 1995
Gamssulzen	<sup>14</sup> C	36,187	533	Pacher & Stuart 2008
Gamssulzen	<sup>14</sup> C	36,239	1,576	Rabeder 1995
Gamssulzen	<sup>14</sup> C	36,603	742	Pacher & Stuart 2008
Gamssulzen	<sup>14</sup> C	38,227	2,452	Rabeder 1995
Gamssulzen	<sup>14</sup> C	41,793	3,102	Rabeder 1995
Gamssulzen	<sup>14</sup> C	42,283	1,671	Rabeder 1995
Gamssulzen	<sup>14</sup> C	44,573	1,019	Pacher & Stuart 2008
Gamssulzen	<sup>14</sup> C	47,676	1,948	Pacher & Stuart 2008
Gamssulzen	<sup>14</sup> C	48,875	2,161	Pacher & Stuart 2008
Gamssulzen	<sup>14</sup> C	48,944	2,302	Pacher & Stuart 2008
Gamssulzen	<sup>14</sup> C	51,256	3,078	Pacher & Stuart 2008

Table 5 List of radiometric dates for the study sites from Rabeder *et al.*, 1995; Rabeder 1995; Rabeder & Withalm, 1995; Pacher & Stuart, 2008; Frischauf & Rabeder (in press).

Crude mean ages for the fossils in the respective caves were calculated on the basis of the youngest and oldest ages (Table 6). For Schwabenreith cave no other dates exist and the Gamssulzen ages are relatively evenly distributed. Short of dating each individual specimen radiometrically, there is no way of knowing the exact age due to disturbance of the sediments by ingress of large quantities of water either by rain or thawing events in spring. This is

obvious from the fact that no fossils are found in situ in the Gamssulzen and Conturines caves. While individuals are still partially undisturbed in Schwabenreith cave they cannot be dated with radiocarbon methods due to their geological age. It is not known for how much of the time represented in the sediment-layer between the two dated sinter layers the cave was actually occupied by cave bears.

Site	Age Range in years	Mean Age in years	Period
Gamssulzen cave	51,256 – 25,400	40,075	Middle Würmian
Conturines cave	115,800 – 41,900	78,850	Early Würmian
Schwabenreith cave	116,000 – 78,400	97,200	Early Würmian

Table 6 Mean age for specimens in each cave. Calculated based on min. and max. ages.

## 2.2) Species

Cave bears (*Sensu lato*) were part of the European megafauna during the late Pleistocene. The genetic convergence date with modern brown bears (*Ursus arctos*) has been calculated to 1.2 to 1.7 million years (Loreille *et al.*, 2000; Hofreiter *et al.*, 2002). They are descendants of the *Ursus deningeri* group, splitting from the lineage that leads to *Ursus spelaeus* between 600,000 years BP (*Ursus ingressus*) and 300,000 years BP (*Ursus ladinicus*) (Rabeder *et al.*, 2000; Hofreiter *et al.*, 2002). *Ursus spelaeus* (*Ursus eremus* and *U. ladinicus*) became extinct 28,500 BP (Bocherens *et al.*, 2013), while *U. ingressus* survived until 15,000 BP (Rabeder *et al.*, 2008).

There is no indication of interbreeding between these three species of cave bears (Hofreiter *et al.*, 2004). In times of geographic co-occurrence they can be separated by the elevation of their habitat. Populations of *U. eremus* and *U. ladinicus* that are found at higher elevations are usually smaller in body size (Rabeder *et al.*, 2008). This ‘alpine nanism’, while common in alpine species (Ehrenberg 1929; Rabeder *et al.*, 2008), cannot be observed in *U. ingressus*. Instead Rabeder *et al.* (2008) suggested that *Ursus ingressus* were able to survive longer in the Alps due to better masticatory performance, as indicated by higher dental morphological indices and evolutionary levels as described in Rabeder (1999).

While *Ursus ingressus* is generally accepted as a separate species (Hofreiter *et al.*, 2004; Rabeder & Hofreiter, 2004), *Ursus eremus* and *U. ladinicus* are sometimes considered subspecies of *Ursus spelaeus* (Hofreiter *et al.*, 2002; Hofreiter *et al.*, 2004).

The individual ages of cave bears have been calculated by counting tooth-cement rings on tooth roots (Debeljak, 1996). A large number of heavily worn teeth can be found, showing individual ages of upwards of 30 years (Rabeder *et al.*, 2000). A recent study has shown that there are significant differences in individuals among the species found at different locations. Furthermore, differences in abrasion rate and stable isotope  $^{13}\text{C}$  content in their bones support the argument of differences in diet among cave bear species, and even between different caves populated by the same species (Holland, 2013). Further studies and additional stable isotope analyses are necessary to establish a more detailed picture and to possibly reconstruct the cave bear paleo-environment.

It has been shown that high-alpine cave bears have a reduced body size. This alpine nanism was first proposed by Ehrenberg (1929) and later corroborated by Kurtén (1955). Later studies supported these findings qualitatively but showed that this was only the case for *Ursus eremus* and *U. ladinicus*. *Ursus ingressus*, on the other hand, does not exhibit any nanism in higher elevations but instead has more-developed molars (Rabeder *et al.*, 2008).

While it is not possible to tell which species of cave bears hibernated in any specific cave from a single tooth just by analyzing the morphology, having a large sample allows making the same distinctions as using destructive genetic sampling. Generally there is a large overlap in evolutionary levels of the teeth between the species and over time (Rabeder, 1999). Given a large enough sample size it is possible to calculate an evolutionary level for any given site and species.

Hofreiter *et al.* (2002) recognized four different haplogroups among cave bears: *Ursus ingressus*, *U. spelaeus spelaeus*, *U. spelaeus ladinicus* and *U. spelaeus eremus*. No indicators of interbreeding have been found, even in locations where they lived contemporaneously for several thousands of years, as in the Lohnetal caves: Hohle Fels, Sirgenstein and Geissenklösterle (Rabeder, personal communication).

### **2.2.1      *Ursus eremus***

The type locality for *Ursus eremus* is Ramesch bone cave (Rabeder *et al.*, 2004). This species has a smaller body size than the geologically coeval *U. ingressus*. According to Rabeder *et al.* (2004) its first metacarpal and metatarsal (Mc1, Mt1) are thicker than those of the type

specimen's population at Zoolith cave, Germany. The dental morphological indices are lower than those of the Conturines population (*U. ladinicus*).

### **2.2.2      *Ursus ladinicus***

The type locality for *Ursus ladinicus* is Conturines cave (Rabeder *et al.*, 2004). This species is usually found in high-alpine caves (Rabeder *et al.*, 2004) and are the species that has been found in the highest elevated location. Recently, however, this species also has been found in less elevated terrain (Rabeder & Withalm, 2011). Generally this species is relatively small in body size and has a more primitive dentition (small dimensions; P3 retained in 25-30% of all specimens; primitive i1 and m2), but with a few modern aspects (i2; m1 and m2 enthyponid highly evolved, as well as highly evolved morphotypes for m2 mesolophid, M<sup>2</sup> metaloph and P<sup>4</sup>) (Rabeder *et al.*, 2004; Rabeder & Hofreiter 2004; Withalm, 2008). The first metacarpal and metatarsal are thick; they are similar to those of *U. eremus* (Withalm, 2001); and they are considered to be an adaptation to a life in high alpine localities.

### **2.2.3      *Ursus ingressus***

The type locality for *Ursus ingressus* is Gamssulzen cave (Rabeder *et al.*, 2004). The caves, which this species frequented, are located in low to medium elevation in the Alps (Rabeder, 2007). This species is relatively larger than the other cave bears. While the other cave bears display alpine nanism in higher elevations, this is not the case with *U. ingressus*. Instead, populations at higher elevations tend to have more highly-evolved teeth (Rabeder *et al.*, 2008). The level of dental evolution, especially the P3, is usually higher than in other cave bears. The P4/4 index is much higher than in the type locality of cave bears (*U. spelaeus*) at Zoolith cave. The metapodials (especially Mc1 and Mt1) are much slimmer than in the Ramesch and Conturines bears (Withalm, 2001; Rabeder *et al.*, 2004). Molecular genetic analysis and a generation time estimate of 10-17 years result in a divergence date of *U. ingressus* from the other cave bears approximately 600,000 years ago (Hofreiter *et al.*, 2002).

### 2.2.4) Genetic Analysis

Collagen, containing ancient DNA, is conserved very well in cave sediments due to the constant cold temperature and high humidity. Genetic analyses are often successful in bones and teeth up to about 100,000 years BP (Rabeder *et al.*, 2004).

A region of approximately 285 base pairs of mitochondrial DNA (mtDNA), from hypervariable region 1, was amplified and a consensus tree was constructed by Hofreiter *et al.* (2002).

While cave bears (*Ursus spelaeus sensu lato*) were considered a very variable species for quite some time (e.g. Ehrenberg, 1931; Temmel, 1996), especially considering the smaller high-alpine forms (Ehrenberg, 1929; Kurtén, 1955), genetic analyses showed that cave bears (*sensu lato*) consisted of at least 2 different species: *Ursus spelaeus* and *U. ingressus* (Rabeder *et al.*, 2004). *Ursus spelaeus* is comprised of three subspecies, *U. spelaeus spelaeus*, *U. spelaeus ladinicus* and *U. spelaeus eremus*, which could possibly be elevated to species level, and are in fact considered as such by some (e.g. Rabeder *et al.*, 2006b; Rabeder *et al.*, 2008; Rabeder & Withalm, 2011).

This study will treat them as separate, though closely related, species as well, due to the fact that they did not interbreed even in locations where both species lived contemporaneously and hibernated in caves separated by only a few kilometers (Hofreiter *et al.*, 2002; Rabeder *et al.*, 2004). While there is no indication of gene flow in either mtDNA or morphology between the populations of Ramesch bone cave and Gamssulzen cave, which are only 10 kilometers apart, more closely related populations are found in similar elevations but located much further apart (Rabeder *et al.*, 2004).

### 2.2.5) Body Size

To approximate body size with high certainty, length measurements can be taken on several elements. To ensure that the body size is neither overestimated nor underestimated by choosing the wrong element for the extrapolation, it is usually safer to include more elements and measurements and compare the estimated body size results. Otherwise, a change in one element's length, width, or circumference due to adaptation to certain environmental

influences could be misconstrued as a change in body size. For this study only metapodial length will be used to approximate body-size. All measurements were collected by Dr. Gerhard Withalm and the results were published in his dissertation thesis (Withalm, 2001). In his thesis Dr. Withalm measured the maximum length of metacarpals and metatarsals.

For this study all metacarpal and metatarsal elements were combined into a mean metacarpal and a mean metatarsal value, respectively. This value reflects the overall size of these elements and neglects differences in individual elements. These measurements have to be used with caution if used to approximate body-size. Withalm (2001) argues that the metapodials are indeed subject to adaptation. Thus the actual differences in mean metacarpal and metatarsal length will not be used, but rather they will be used to rank these three cave bear species by relative body-size. As can be seen in Table 7 the Gamssulzen and Schwabenreith bears are approximately the same size, while the Conturines individuals are notably smaller.

	<b>CU</b>	<b>GS</b>	<b>SW</b>
<b>Mt mean length (mm)</b>	69.84	73.54	74.7
<b>Mt variance</b>	195.933	183.628	174.695
<b>Mc mean length (mm)</b>	73.26	76.62	76.74
<b>Mc variance</b>	53.563	68.517	61.083

Table 7 Mean metapodial size measurements for the 3 populations based on mean measurements for each element (Withalm, 2001).

## 2.3) Element and Sample

This study will focus on the upper 2<sup>nd</sup> molar. The general carnivore dental trait, the enlarged carnassials, results in a reduction in molar teeth size or a loss of posterior teeth. In ursids, the carnassials are the maxillary 4<sup>th</sup> premolar and the mandibular 1<sup>st</sup> molar. To create room for the large carnassial teeth in ursids, the upper 3<sup>rd</sup> molar is lost. As cave bears are herbivorous, their carnassials were reduced and the upper 2<sup>nd</sup> molar was elongated instead, to interact with both the lower 2<sup>nd</sup> and 3<sup>rd</sup> molars. In other bears, the 3<sup>rd</sup> upper and lower molars are usually smaller than the 2<sup>nd</sup> molars. Since the most distal teeth are the least constrained in terms of neighboring structures they became elongated in cave bears. The lower 3<sup>rd</sup> and the upper 2<sup>nd</sup> molars increase in size, thus creating a larger surface area to grind their tough diet.

Omnivory has been considered for cave bear populations in at least two caves. It has been argued that at Pesteră cu Oase (Romania) cave bears were omnivorous on the basis of higher Nitrogen isotope values (Richards *et al.*, 2008), while microwear analyses from Goyet (Belgium) indicate a period of predormancy omnivory (Peigne *et al.*, 2009).

The upper 2<sup>nd</sup> molar also shows a high intraspecific variability (Rabeder, 1999). Rabeder *et al.* (2008) and Rabeder and Withalm (2011) calculated sex indices (following Rabeder, 2001) for several cave sites, based on canine dimensions. The female-to-male ratio differs among the three studied sites (Table 8). They calculated an even ratio at Conturines, but substantially more females at Gamssulzen and Schwabenreith (73.49 % and 64.56 %, respectively). The same ratios can be assumed for the elements in this study, but cave bear molars do not show pronounced sexual dimorphism (Kurtén, 1955) so this disparity can be ignored.

Site	Species	Sex Index (% of females)
Schwabenreith cave	<i>U. eremus</i>	64.56
Gamssulzen cave	<i>U. ingressus</i>	73.49
Conturines cave	<i>U. ladinicus</i>	53.61

Table 8 Sex indices based on canine dimensions as published by Rabeder & Withalm, 2011.

Since the applied methods allow for mirrored data, both left and right sided elements will be included in the analysis. The sample is comprised of at least nine specimens per species to capture the variability of shapes. All teeth in this study are isolated teeth; none show serious wear and most are tooth germs without fully formed roots. The only criteria they were selected for were an absence of wear or large cracks. The molars from Gamssulzen cave are generally the largest of the studied sample, while those from Conturines cave were the smallest (Table 9, Figure 1). The standard deviations for the three subsamples are very similar to one another. Their mean length and width are representative of the Conturines and Gamssulzen cave populations for which larger samples have previously been measured (Rabeder *et al.*, 2004). The Conturines M<sup>2</sup> length standard deviation in the sample used in this study is larger than for the whole sample (Std. Dev. = 1.49; Rabeder *et al.*, 2004).

Species	Mean Length (mm)	Std. Dev.	Mean Width (mm)	Std. Dev.
<i>Ursus ingressus</i>	43.62	2.60	22.52	1.64
<i>U. eremus</i>	42.60	2.25	21.87	1.40
<i>U. ladinicus</i>	40.84	2.15	20.93	1.36

Table 9 Linear measurements. Mean maximal length and width for each location subsample.

CU\_29-2



SW\_194-3



GS\_157-1



Figure 1 Occlusal view of 3 specimens representing each population. CU (top left); SW (top right, image flipped); GS (bottom left).

### 2.3.1) Length of tooth row p4 – m3

In order to put the shape changes of the  $M^2$ s into context, the length of the mandibular post-canine tooth-rows was estimated. This would also allow a calculation of the relative length of the  $M^2$  in a representative average cave bear jaw. Since very few crania have been excavated



and even fewer have their full premolar and molar dentition still in place it was necessary to measure the antagonist tooth row instead. The mandibular tooth row  $p_4$  to  $m_3$  should, as a structure, have the same total length as the maxillary  $P^4$  to  $M^2$  so as to be functional in occlusion. While the lower  $p_4$  is slightly protruding over the upper  $P^4$ , the opposite is true for the upper  $M^2$  and lower  $m_3$ . Table 10 shows the mean tooth row lengths for each site, measured from  $p_4$  to  $m_3$ . Specimens were sexed on the basis of the canine shape or canine alveoli. Measurements were taken and specimens were sexed by the author specifically for this study. A full list of specimens is available in the appendix (Table 23). All specimens are housed at the Department of Paleontology at the University of Vienna.

Site	Mean length	Total n	Female mean length	Female n	Male mean length	Male n
CU	98.1125	8	93.66667	3	100.78	5
GS	100.259091	22	96.34	10	103.33636	11
SW	98.53	20	96.60714	14	103.01667	6

Table 10 mean lengths of mandibular tooth row  $p_4$  -  $m_3$ .

## 2.4) 3D Models and Programs

### 2.4.1 CT scanner (Vienna Micro-CT Lab)

All specimens were scanned specifically for this study between February and July of 2012 at the Vienna Micro-CT Lab (Viscom X8060, University of Vienna, Department of Anthropology) and at the Department of Paleontology (SkyScan 1173 Desktop-Micro-CT) by trained personnel. Sixteen specimens were scanned on each machine with resolutions varying between 35 and 47 microns (Table 23). Due to technical reasons not all scanned specimens were used. Ten specimens representing Gamssulzen, ten representing Conturines and nine representing Schwabenreith were included.

### 2.4.2 AMIRA (VSG – Visualization Science Group, France)

The scans were segmented using Amira software (version 5.4.5). The enamel cap and dentin were segmented separately to allow for placing landmarks on each structure individually. Due

to irregular fossilization it was not possible to employ the semi-automatic half-maximum height value (HMHV) protocol (Spoor *et al.*, 1993) in all cases and instead segmentation was done mostly slice by slice. The surface files for enamel and dentin were exported separately as .obj files. The curves, on which the semi-landmarks were to be placed later were also created in Amira and exported as .obj files as well.

### **2.4.3 EVAN Toolbox (EVAN-Society e.V.)**

Landmarking was done in the Templand module of the EVAN Toolbox (ET), and the Generalized Procrustes Analysis (GPA) and Principal Components Analysis (PCA) were run in ET. The main landmarks were placed on the respective, homologous structures. Specimen GS\_27 was used as the template file on which the semi-landmarks were first placed roughly equidistant around the curves. After placing the main landmarks on each specimen, the semi-landmarks were projected from the template to the respective curves on the target specimens and slid to minimize bending energy. A network was set up to run a GPA and PCA for form space and shape space to visualize shape changes. A second network was set up for regression analysis.

### **2.4.4 Morphologika 2 (v.2.5)**

Morphologika 2 was used to test for the effects of allometry in this sample. A file containing the coordinates of all landmarks on all specimens was created in ET and exported in Morphologika-rady format. The .txt file was imported into Morphologika 2 where separate GPA and PCA analyses were run for shape space and form space. For the latter no scaling to centroid size was performed. Regressions of shape on centroid size were run separately for each PC.

## 2.5) Landmarks

The landmark set includes 18 landmarks and seven curves with 71 semi-landmarks in total. A similar landmark protocol was first published by Seetah *et al.* (2012) and was adapted for this study to include dentin shape as well.

Landmarks were chosen to include all major cusps and other easily observable structures (Table 11). All landmarks are homologous among the specimens in this study. All major cusps were landmarked on both the enamel and the dentin surface to allow for comparable tests of M<sup>2</sup> shape differences among the three cave bear species.

Landmarks 1 through 7 mark the tips of the six main cusps and the Hypostyle. In cave bears, the Protocone is often separated into two distinct cusps. Protocone I is located mesial to Protocone II. In cases where these landmarks were not easily discernible on the enamel, i.e. the point of highest curvature was not obvious, they were projected from the underlying dentin horn tips. For this a plane was added on the cervical line, which was considered to be representative of the occlusal surface. The tooth was then oriented so that the plane was parallel to the computer screen. The point on the enamel that was directly atop of the dentin landmark was used as the enamel landmark.

Landmarks 8 and 9 on the buccal and lingual crease are located where the deep folds originating in the Trigone intersect with the buccal and lingual crests, respectively. The buccal fold intersects between the Paracone and Metacone and the lingual fold intersects between the Protocone II and the Hypocone. Landmark 10 marks the lowest point in the Trigone between the Paracone, Metacone and Protocone. Landmarks 11 to 17 are located on the tips of the dentin horns underlying the corresponding enamel cusps. Landmark 18, the dentin horn tip underlying the Parastyle, was not represented on the enamel because this feature is almost never visible, but rather integrated into the anterior cingulum.

The definition of landmark types follows Weber and Bookstein (2011), who replaced the original definition of landmarks by Bookstein (1991). Type 2 landmarks are characterized by extremes in curvature. These are the peaks or pits on the surfaces, i.e. cusp tips and the lowest point on the Trigone. Type 3c landmarks are intersections of ridge curves and observed

curves. In this landmark protocol this is how landmarks 8 and 9 are defined. The models were landmarked in a random order to minimize effects of the author becoming accustomed to the element and landmarks. If an increase in landmarking precision developed it will be spread among all three groups, thus reducing bias.

<b>Landmark</b>	<b>Location</b>	<b>Landmark Type</b>	<b>On Structure</b>
1	Paracone (Pa)	2	Enamel
2	Metacone (Me)	2	Enamel
3	Metastyle (Mt)	2	Enamel
4	Protocone I (PrI)	2	Enamel
5	Protocone II (PrII)	2	Enamel
6	Hypocone (Hy)	2	Enamel
7	Hypostyle (Hys)	2	Enamel
8	Buccal Crease (Pa/Me)	3c	Enamel
9	Lingual Crease (PrII/Hy)	3c	Enamel
10	Central pit in Trigone	2	Enamel
11	Paracone	2	Dentin
12	Metacone	2	Dentin
13	Metastyle	2	Dentin
14	Protocone I	2	Dentin
15	Protocone II	2	Dentin
16	Hypocone	2	Dentin
17	Hypostyle	2	Dentin
18	Parastyle	2	Dentin

Table 11 List of Landmarks in this study. Landmark types according to Weber & Bookstein (2011).

The landmarks as well as the seven curves are marked on both the enamel and the dentin surfaces of GS 27-1, the specimen used as the template for this study (Figure 2).

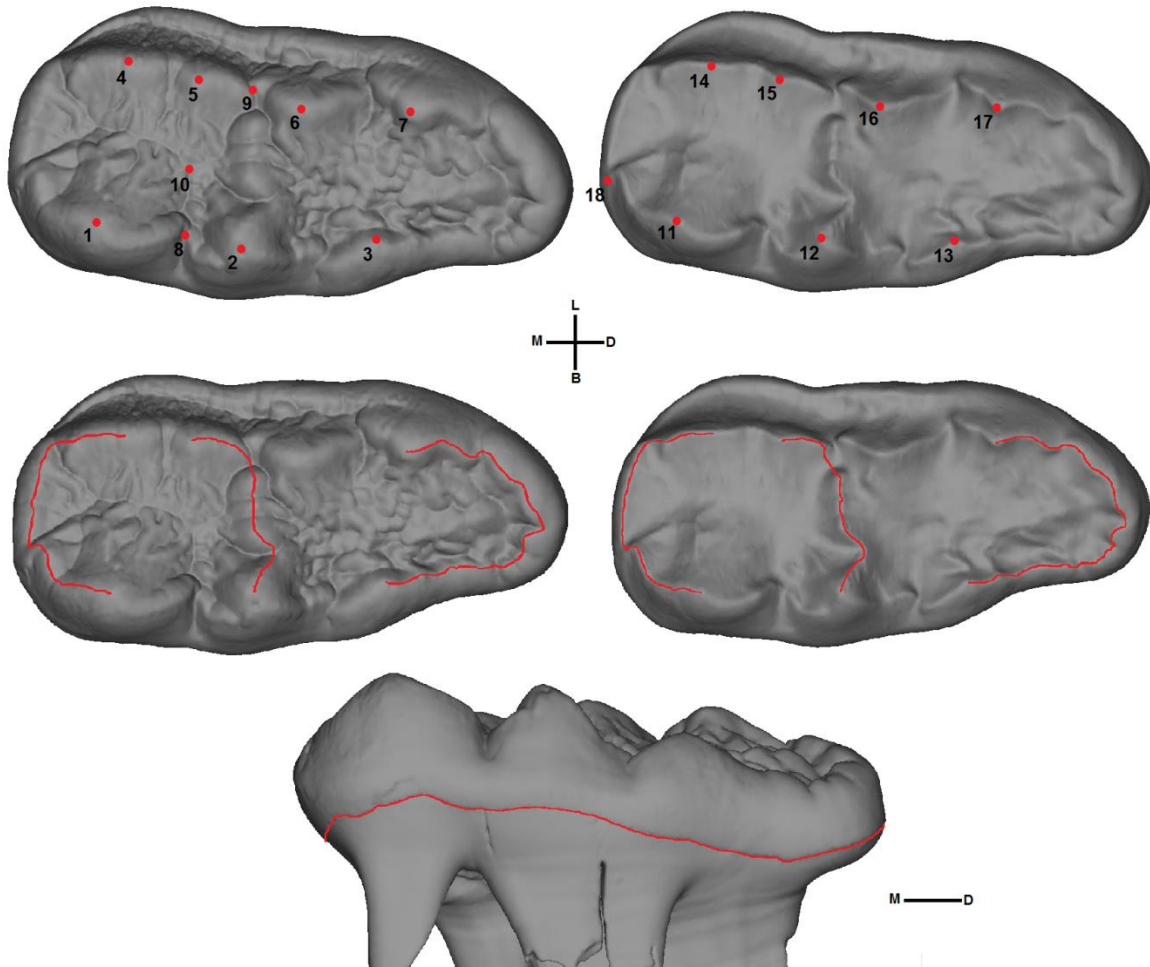


Figure 2 Landmarks on the enamel (upper left) and dentin (upper right) surfaces of GS 27-1 in occlusal view. Curves on the enamel (middle left) and dentin (center right) surface. GS 27-1 in bucco-lateral view with cervical line curve

All curves in this study are homologous biological structures (Table 12). There are three curves along pronounced ridges on the enamel, three along the underlying dentin, and one around the cervical line of the tooth. The curve on the mesial ridge runs between the Paracone and the Protocone I. The talonfield ridge curve runs between the Metastyle and Hypostyle cusps along the distal ridge around the talonfield. The metaloph ridge is more variable. In about two thirds of the sample it runs between the Metacone and the Mesocone (21 out of 32) and in one third of the cases it runs between the Metacone and the Hypocone (11 out of 32). This ratio is representative for all three sites in this study. In the samples of *U. ingressus*, *U. ladinicus* (seven out of 11, each) and *U. eremus* (seven out of ten) roughly two thirds of the metaloph ridges end in the Mesocone. Rather than following the metaloph ridge to the Hypocone, the curve was instead anchored between the Metacone and Mesocone. The same number of evenly spaced semi-landmarks was placed on corresponding curves.

Landmarks	Curve	Delimiting Landmarks	Landmark Type	On Structure
17	Cervical Line Curve	Along Cervical Margin	4	Cervical Line
9	Mesial Ridge	Paracone – Protocone I	4	Enamel
7	Metaph Ridge	Metacone – Mesocone/Hypocone	4	Enamel
11	Talonfield Ridge	Metastyle - Hypostyle	4	Enamel
9	Mesial Ridge	Paracone – Protocone I	4	Dentin
7	Metaph Ridge	Metacone – Mesocone/Hypocone	4	Dentin
11	Talonfield Ridge	Metastyle - Hypostyle	4	Dentin

Table 12 List of Curves and semi-landmarks included in this study. Landmark types according to Weber & Bookstein (2011).

## 2.6) Generalized Procrustes Analysis (GPA) and Principal Components Analysis (PCA)

During a Generalized Procrustes Analysis (also known as Procrustes Superimposition) all shapes are scaled, rotated, and translated so as to minimize the overall sum of squares value. To do this, the mean shape is calculated from the whole sample and used as a reference shape to which all other shapes are aligned. The other shapes are oriented in a way that the square root of the sum of the squared distances between each corresponding landmark is as small as possible.

This technique transfers the objects from figure space to Kendall's shape space. A superimposition of shapes that only includes rotation and translation, but does not scale them, transfers the shapes into form space. In most cases form space will be dominated by a large influence of size on the first principal components axis (PC1).

The aligned data is then submitted to a Principal Components Analysis. This function realigns the multidimensional cloud to be more easily represented in a two-dimensional medium. In order to do so, the first axis (PC1) is defined by passing through the highest variance of the point cloud. The second axis (PC2) has to be orthogonal to the first axis and has to pass

through the highest variability possible. In choosing orthogonal axes it can be guaranteed that the variance shown is uncorrelated. All further axes follow the same rules.

As many principal components axes are created as there are dimensions of variation within the dataset. The number of dimensions for a particular landmark protocol are  $3p-7$  for a three dimensional dataset; where  $p$  = the number of landmarks. Seven dimensions are subtracted because they are being held constant (three for translation and rotation each, and one for size) during GPA. Partial warp scores are calculated for each principal component to characterize the location of every landmark in the multidimensional space.

## 2.7) Regression of PC Scores on Centroid Size

### 2.7.1 Centroid Size

Centroid size is the square root of the sum of squared distances between a set of landmarks and the centroid of an individual. This variable can be used to represent the size of a specimen as it is uncorrelated with the shape variables. Correcting for centroid size holds the size of all specimens constant in a GPA, which allows for visualization of differences in shape and removes differences in size. The Principal Component Analysis based on these data is located in shape space.

### 2.7.2 Allometry

Allometry is the change of shape with differences in size. Almost all animals change their shape during growth. If shape does not change with size this is called isometry and simply shows a larger version with the same ratios. Regression of principal warp scores on centroid size visualizes the correlation of shape changes with body size, thus indicating the role of size in the differences of shape. The RV-coefficient is the measure that shows the influence of size on shape, with a higher RV-coefficient indicating more influence (Robert & Escoufier, 1976).

## 2.8) Canonical Variance Analysis (CVA)

A Canonical Variance Analysis is a special Multivariate Analysis of Variance (MANOVA). It calculates a linear function that increases between-group variability in relation to within-group variability for pre-determined groups in a dataset. This is done by calculating the Mahalanobis distance between each individual's principal component scores and the mean group principal component scores. One basic assumption for this analysis is the similar variability for each of the included groups, which has to be tested beforehand. The CVA calculation was run using PAST software (Hammer *et al.*, 2001).

## 3) Results

### 3.1) Centroid Size

The centroid size for each specimen and the group mean sizes are listed in Table 13. The range of centroid size is very similar among the groups (Figure 3, Table 14). Variance is largest within *Ursus eremus* (SW) and lowest within *Ursus ingressus* (GS). Although there is a difference in mean centroid size between the groups, this difference is not significant ( $p=0.22$ ) as shown in Table 15.

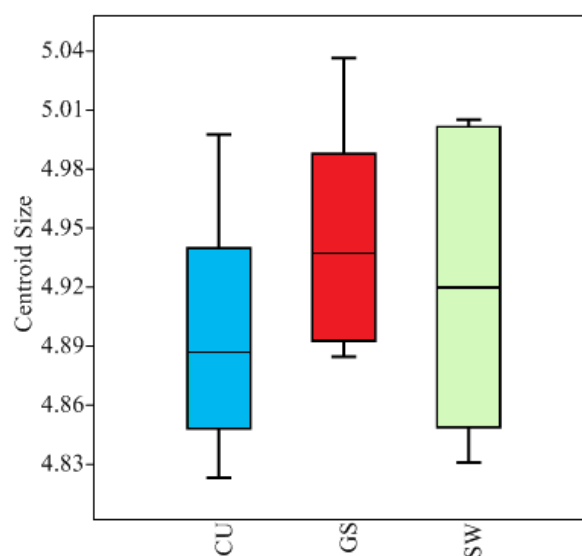


Figure 3 Boxplot of centroid size showing the large overlap among species.  
Whiskers show standard deviation.



Specimen	Centroid Size	Group Mean CS	Specimen	Centroid Size	Group Mean CS
CU_1-2	4.86545	CU = 4.89660	GS_12-3	5.00284	GS = 4.94293
CU_4-1	4.82311		GS_26-3	4.90274	
CU_6	4.92921		GS_38-1	4.93581	
CU_14-1	4.88685		GS_27-1	4.95800	
CU_21-2	4.87074		GS_109-1	4.9878	
CU_29-2	4.96796		GS_147-3	4.93732	
CU_38-2	4.84819		GS_148-1	4.89271	
CU_53-2	4.93977		GS_159-1	5.03649	
CU_55-1	4.99751		GS_194-2	4.88472	
CU_31-1	4.83725		GS_197-1	4.89095	
SW_194-3	4.91993	SW = 4.92263			
SW_359-1	5.00511				
SW_382-9	4.95014				
SW_468-5	4.95992				
SW_789-8	4.84888				
SW_882	4.91941				
SW_1032-4	4.83086				
SW_1706	4.86820				
SW_1869	5.00124				

Table 13 Centroid Size for each specimen and group mean.

Groups	Count	Min	Max	Mean	Variance
CU	10	4,82311	4,99751	4.89660	0.00347
GS	10	4,88472	5,03649	4.94294	0.00277
SW	9	4,83086	5,00511	4.92263	0.004

Table 14 Variation of centroid size for all three groups.

Source of Variance	Sum of Squares	Degrees of Freedom	Mean Sum of Squares	F-value	p-value	Critical F value
Between Groups	0,010785011	2	0,00539	1,59203	0,22272	3,36902
Within Groups	0,088066778	26	0,00339			
Total	0,098851789	28				

Table 15 Results of ANOVA of centroid size.

All relevant size measurements used in this study are summarized in Table 16. The only size values that are significantly different between the groups are the mean tooth length ( $p=0.04988$ ) and tooth length variance ( $p=0.03706$ ), showing that the Conturines bears are much more restricted in the variability of their tooth length than the Gamssulzen bears, and slightly more so than the Schwabenreith bears. The Gamssulzen bears show a wider range of tooth width measurements, although these results are not statistically significant.

	CU	GS	SW	ANOVA p=
<b>Centroid size</b>	4.89660	4.94294	4.92302	
<b>Centroid size variance</b>	0.003467	0.002766	0.004	0.22241
<b>Mt mean length</b>	69.84	73.54	74.7	
<b>Mt variance</b>	195.933	183.628	174.695	0.84209
<b>Mc mean length</b>	73.26	76.62	76.74	
<b>Mc variance</b>	53.563	68.517	61.083	0.73245
<b>Mean tooth length</b>	40.731	43.627	42.81111	0.04988
<b>Tooth length variance</b>	4.98428	7.50409	5.19471	0.03706
<b>Mean tooth width</b>	20.874	22.545	21.81	0.1117
<b>Tooth width variance</b>	2.00763	2.97958	2.15133	0.0709

Table 16 Various size measurements for the 3 populations, including measurements by Withalm, 2001.

### 3.2) $M^2$ /post-canine tooth row ratio

The measured mandibulae do not show the same sex-ratio as have been calculated on the basis of canines alone (Rabeder & Withalm, 2011). Mean post-canine tooth row lengths were calculated by weighing the mean female and male tooth-row lengths according to the percentage of each sex at the overall site. The weighed mean lengths differ slightly from the un-weighed means (Table 17).

Site	Un-weighed mean tooth-row length	Weighed mean tooth-row length
CU	98.1125	96.96654
GS	100.2591	98.19474
SW	98.53	98.87868

Table 17 Weighed and un-weighed mean lengths of post-canine mandibular tooth-rows for each site.

The proportionate length of the  $M^2$  to the total post-canine tooth-row length is listed in Table 18. While the percentage that the  $M^2$  accounts for in total post-canine tooth-row length is not much different among the three groups, the lowest is found in the bears from Conturines cave (42%) and highest in the Gamssulzen bears (44%).

Site	Proportionate length of $M^2$ to post-canine tooth row
CU	0.42118
GS	0.44422
SW	0.43083

Table 18 Proportionate length of  $M^2$  to weighed post-canine tooth row length for each site.

### 3.3) PCA in Shape Space

Table 19 shows the Principal Components and the amount of shape variation they account for in this sample. The first seven Principal Components cumulatively account for 72.5% of the variation. The most prominent shape changes along those seven Principal Component axes will be described below. The other Principal Components following those seven each account for less than 5% of overall variation and will not be discussed.

Principal Component	Eigenvalues	Variance (%)	Cumulative Variance (%)
PC 1	0.00116	21.93770	21.93770
PC 2	0.00076	14.29430	36.23200
PC 3	0.00054	10.15680	46.38880
PC 4	0.0004	7.49368	53.88250
PC 5	0.00037	6.94442	60.82690
PC 6	0.00033	6.30888	67.13580
PC 7	0.00028	5.39042	72.52620
PC 8	0.00018	3.42516	75.95140
PC 9	0.00015	2.91902	78.87040
PC 10	0.00015	2.82920	81.69960
PC 11	0.00013	2.51007	84.20970
PC 12	0.00011	2.08128	86.29100
PC 13	9.69E-05	1.83349	88.12440
PC 14	8.94E-05	1.69263	89.81710
PC 15	7.54E-05	1.42707	91.24410
PC 16	7.46E-05	1.41099	92.65510
PC 17	6.00E-05	1.13495	93.79010
PC 18	5.95E-05	1.12606	94.91610
PC 19	4.46E-05	0.84443	95.76060
PC 20	4.07E-05	0.77021	96.53080
PC 21	3.29E-05	0.62325	97.15400
PC 22	2.93E-05	0.55506	97.70910
PC 23	2.77E-05	0.52380	98.23290
PC 24	2.30E-05	0.43474	98.66760
PC 25	2.11E-05	0.39971	99.06730
PC 26	2.08E-05	0.39437	99.46170
PC 27	1.58E-05	0.29853	99.76020
PC 28	1.27E-05	0.23977	100.00000

Table 19 Principal Components in Shape Space with the amount of variance they contribute to shape.

At first glance the mean shapes, morphed from the template specimen (GS-27), do not show much difference (Figure 4). In order to visualize shape changes along the PC axes two points on + 0.1 and on – 0.1 will be shown while the value on the other axes will be kept at 0. The visualization of theoretical shapes further along the respective axes will amplify shape

changes and make small differences visible. Each PC axis following the first two will be plotted against PC1.

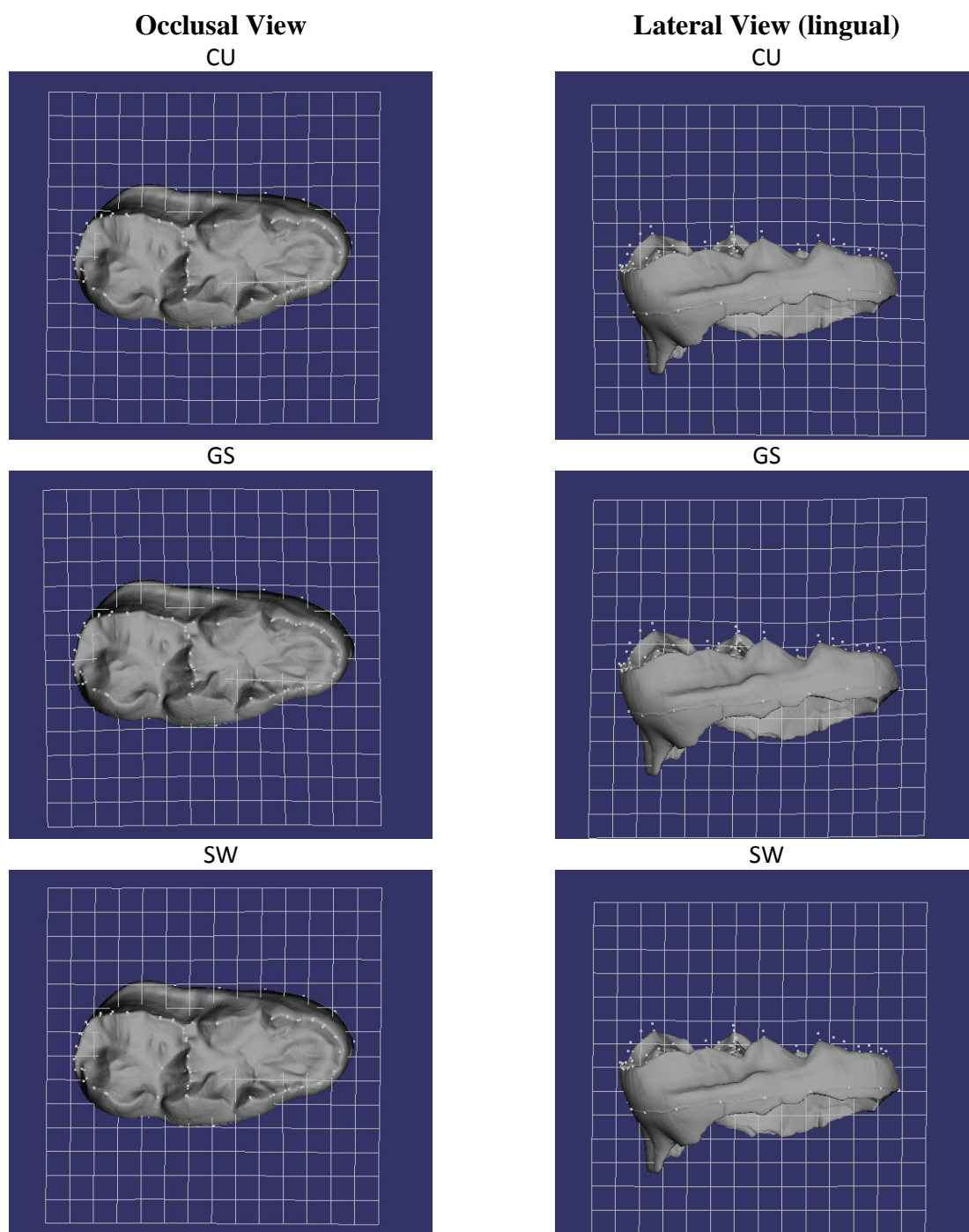


Figure 4 Mean specimens for each population in occlusal (left) and lateral view (right). Warped structure shows dentin surface, all landmarks and thin plate spline grid.

PC1:

The best separation is visible along PC1, which accounts for approximately 22% of variation and separates the Conturines group from the Gamssulzen group (Figure 5). Conturines and

Gamssulzen specimens do not vary much along this axis within their group. Although the majority of Schwabenreith specimens also cluster closer with the Conturines group, some outliers have values within the range of Gamssulzen individuals (#25 and #26). The Schwabenreith group extends far along both positive and negative values on PC1, with specimens #21 and #26 almost at the most extreme ends of the axis.

Specimens with a more positive PC1 value are straighter with a relatively further distally located Metaloph (Figure 6). Those with a negative value are convex both buccally and in occlusal view. The Talonid is thus curved downward and lingual.

PC2:

The PC2 axis (Figure 5) does not show a good separation of the groups. Rather, they show similar strong variability, with the Schwabenreith group showing more positive values than the others. This Principal Component accounts for approximately 14% of the total shape variation. The Talonid becomes broader with more positive PC2 values, and more wedge-shaped with negative values (Figure 7). Along with becoming broader, the teeth also become more planar and thus the cervical line is less twisted.

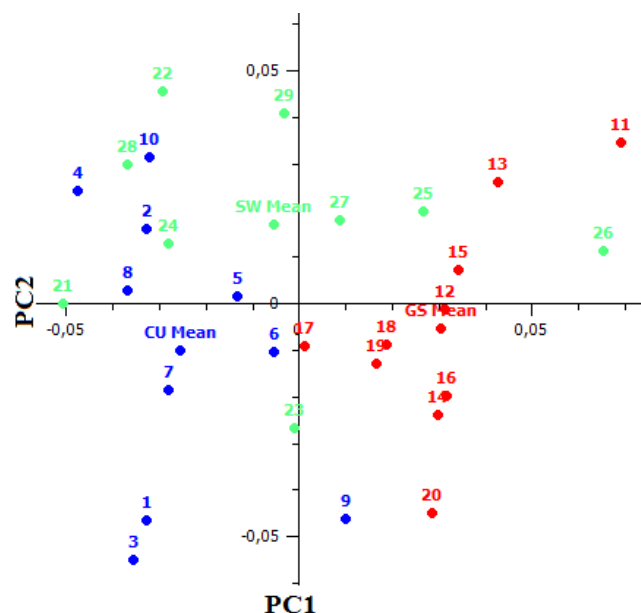


Figure 5 PC1 vs. PC2 in shape space.

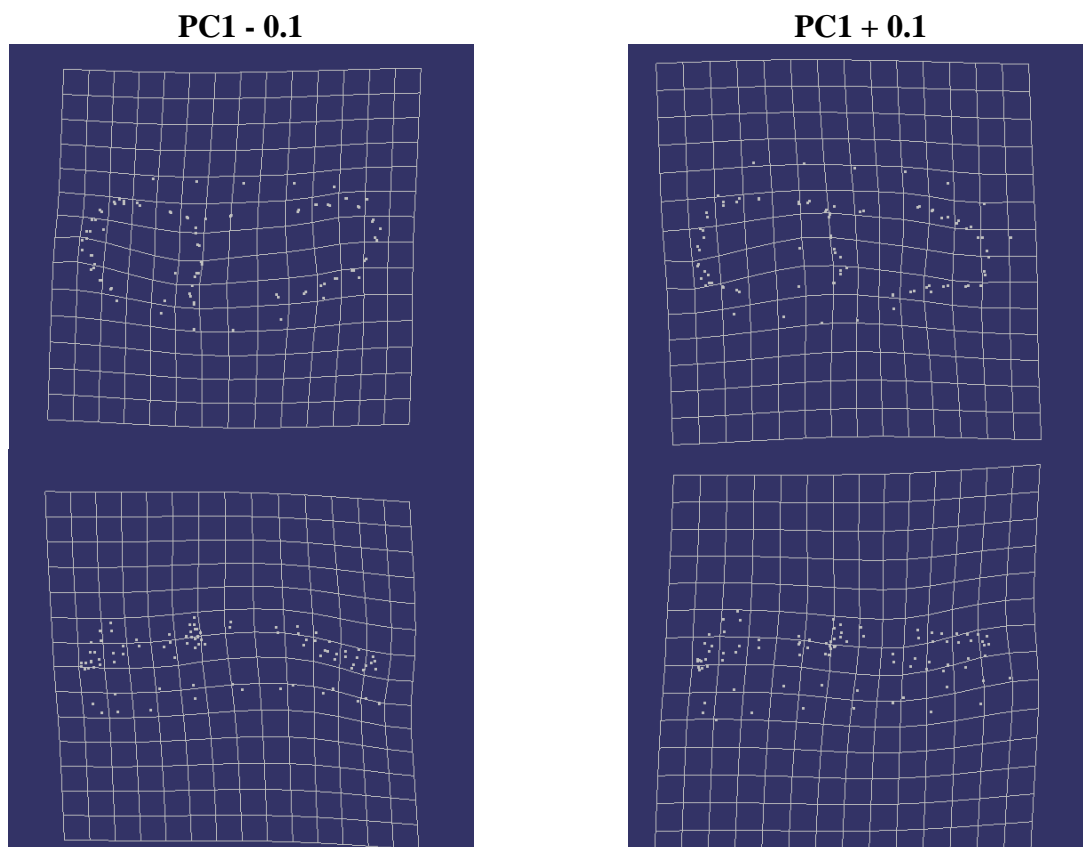


Figure 6 Thin plate spline and location of landmarks in occlusal (first row) and lateral view (second row) along PC1 axis at -0.1 and +0.1, showing the hot-spots of shape change along this axis.

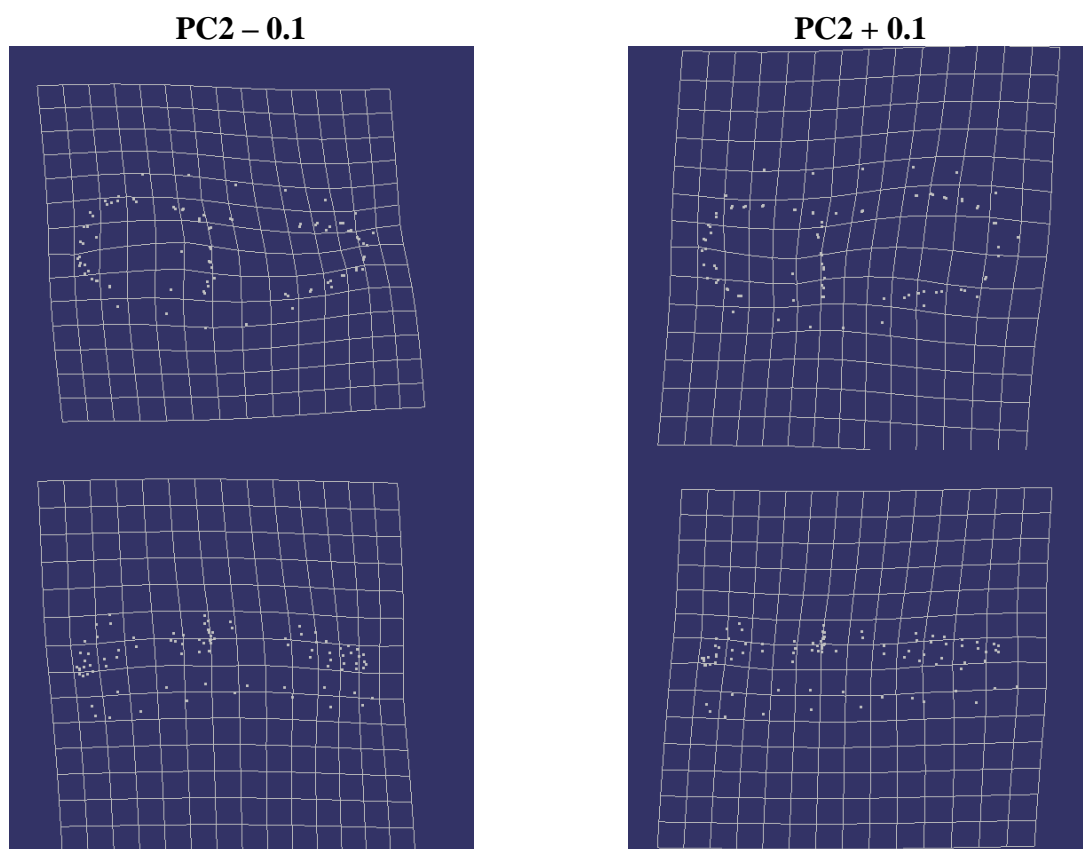


Figure 7 Thin plate spline and location of landmarks in occlusal (first row) and lateral view (second row) along PC2 axis at -0.1 and +0.1, showing the hot-spots of shape change along this axis.

PC3:

PC3 (Figure 8) accounts for approximately 10% of the variation in the entire sample. The bulk of the Conturines group shows little variation along this axis and the groups do not separate well. With more positive values, the Protocone 1 and Hypostyle are located further mesial while the Metastyle moves distally (Figure 9). Thus the Hypocone and Protocone 2 are situated closer together and the Mesial ridge becomes shorter while the Talonid ridge becomes elongated on the lingual side. With more negative values, the lowest point in the Trigonid is much deeper.

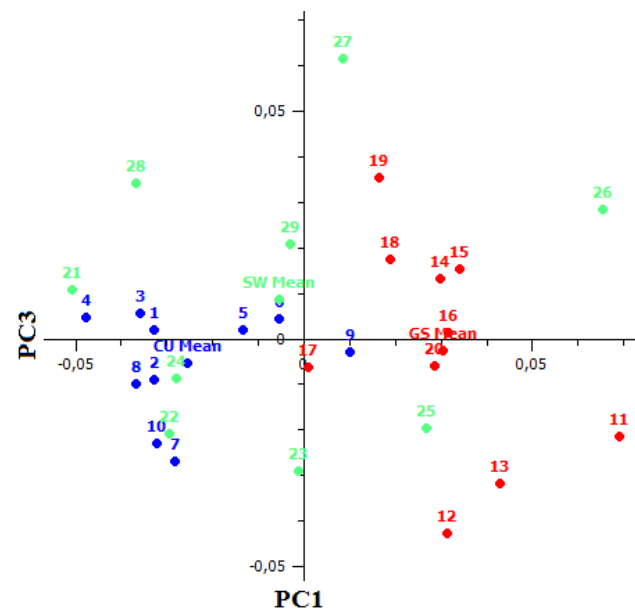


Figure 8 PC1 vs. PC3 in shape space.

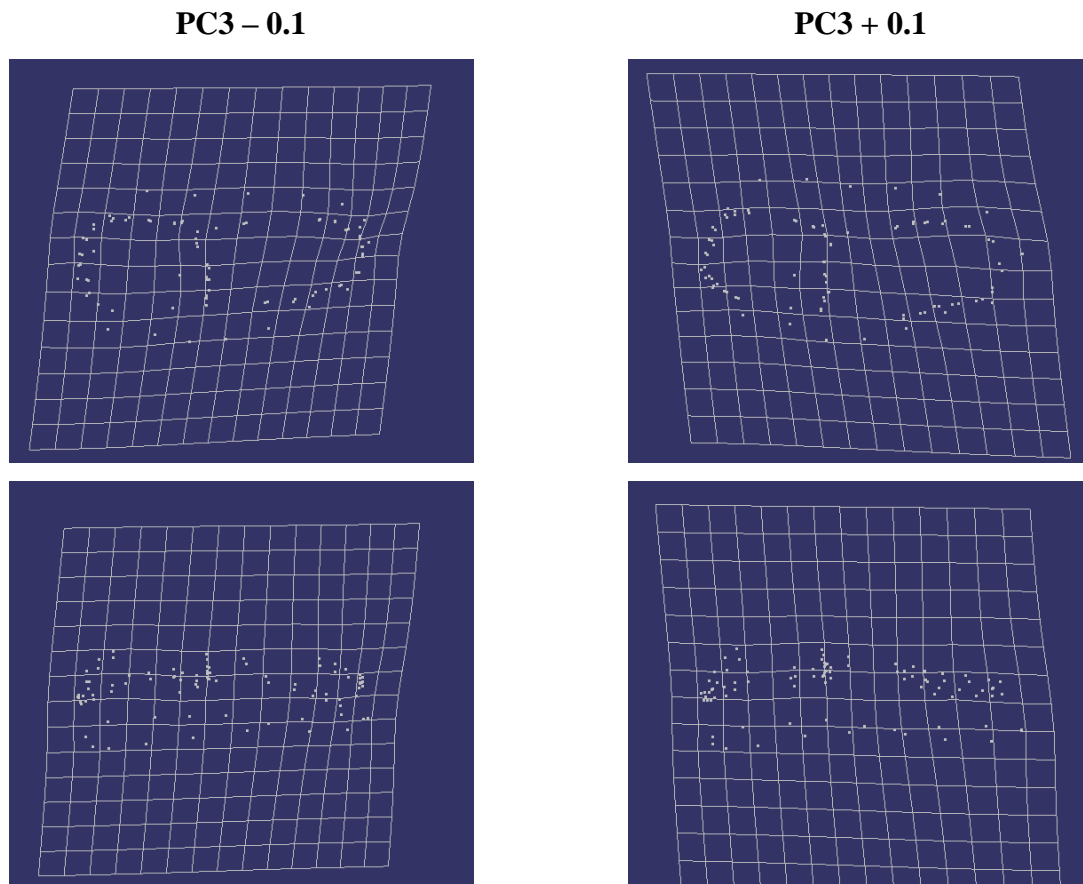


Figure 9 Thin plate spline and location of landmarks in occlusal (first row) and lateral view (second row) along PC3 axis at -0.1 and +0.1, showing the hot-spots of shape change along this axis.

PC4:

The groups do not separate along the PC4 axis. The Gamssulzen and Conturines groups appear to cluster more tightly than the Schwabenreith group, but all show some variation (Figure 10).

With stronger negative values Protocone 1 and 2 move closer together, the mesial ridge becomes more squared and elongated and the Metaloph is located further mesial (Figure 11). Also, the lowest point of the central fossa moves further buccally and the Talonid becomes wedge-shaped. With more positive values the Talonid becomes squared and the mesial ridge is shortened.



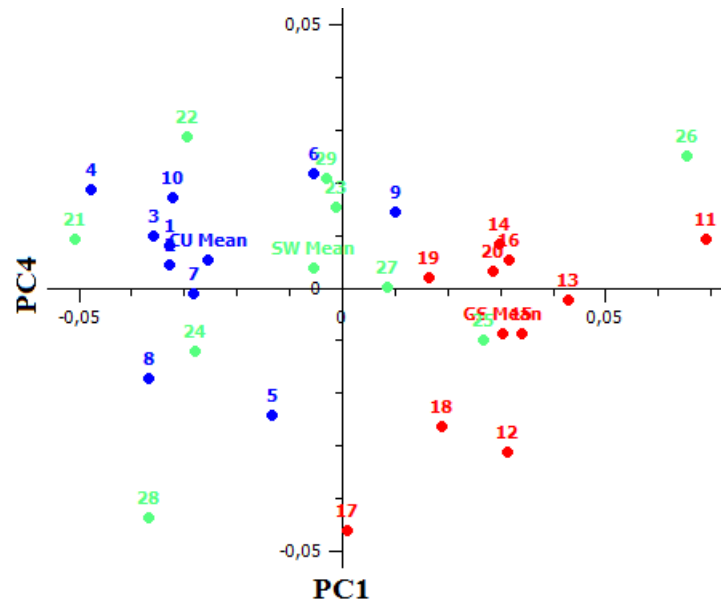


Figure 10 PC1 vs. PC4 in shape space.

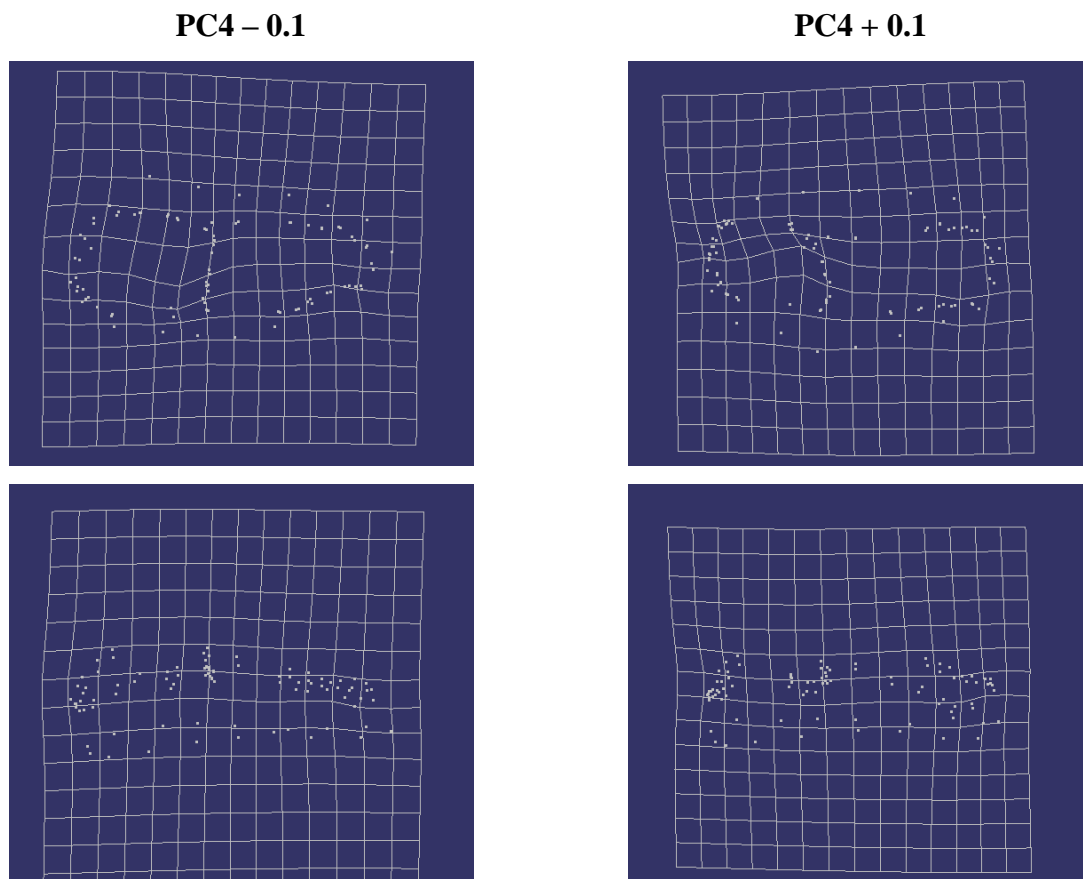


Figure 11 Thin plate spline and location of landmarks in occlusal (first row) and lateral view (second row) along PC4 axis at -0.1 and +0.1, showing the hot-spots of shape change along this axis.

PC5:

The groups do not separate along this axis (Figure 12). The Schwabenreith group shows less variation than the other two. In occlusal view the individuals with a more positive PC5 value are more convex on the lingual side (Figure 13). The occlusal surface becomes narrower and the dentin cusps become taller. The hypostyle moves away from the Hypocone towards the distal end and the lowest point of the central fossa moves buccally. The distal part of the talonfield becomes larger. With more negative values the tooth becomes much broader and flatter and the lingual cingulum is more bulging.

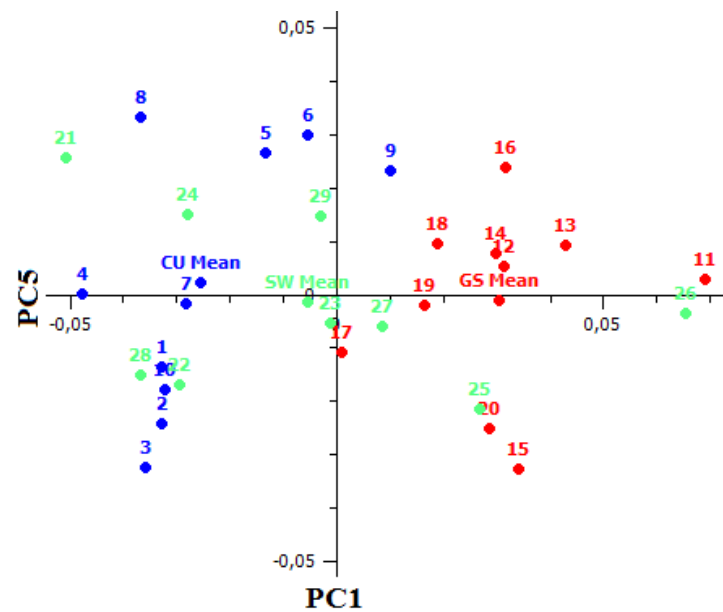


Figure 12 PC1 vs. PC5 in shape space.

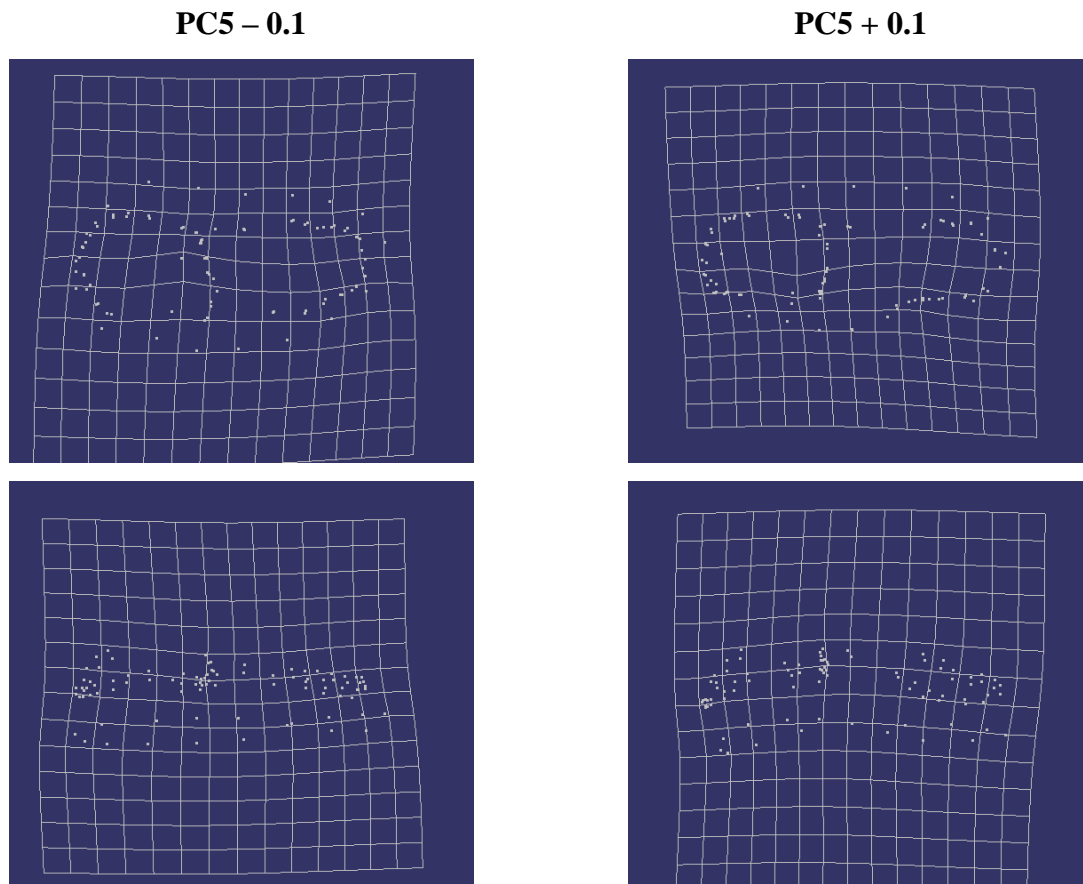


Figure 13 Thin plate spline and location of landmarks in occlusal (first row) and lateral view (second row) along PC5 axis at -0.1 and +0.1, showing the hot-spots of shape change along this axis.

#### PC6:

The Conturines and Gamssulzen groups, although overlapping, show slight separation and clustering of specimens along PC6 (Figure 14). The Schwabenreith specimens overlap with both groups. With stronger negative values the tooth cusps move closer to the center of the occlusal surface and give the tooth a more “streamlined” look (Figure 15). The Metaloph drops lower in relation to the other cusps, especially compared to the taller Metacone and Hypocone. The Hypocone moves mesially, and the lowest point of the central fossa is located more buccally. With more positive values Protocone 1 and 2 move closer together, the Metastyle drops lower and the Hypocone moves more lingually, moving out of line with the other lingual cusps. In general the tooth, especially the talonfield, becomes broader and the cusp height is reduced.

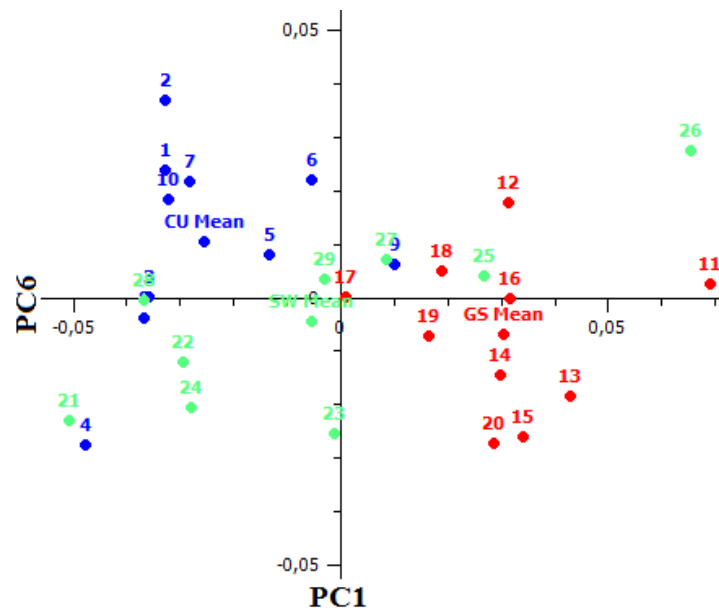


Figure 14 PC1 vs. PC6 in shape space.

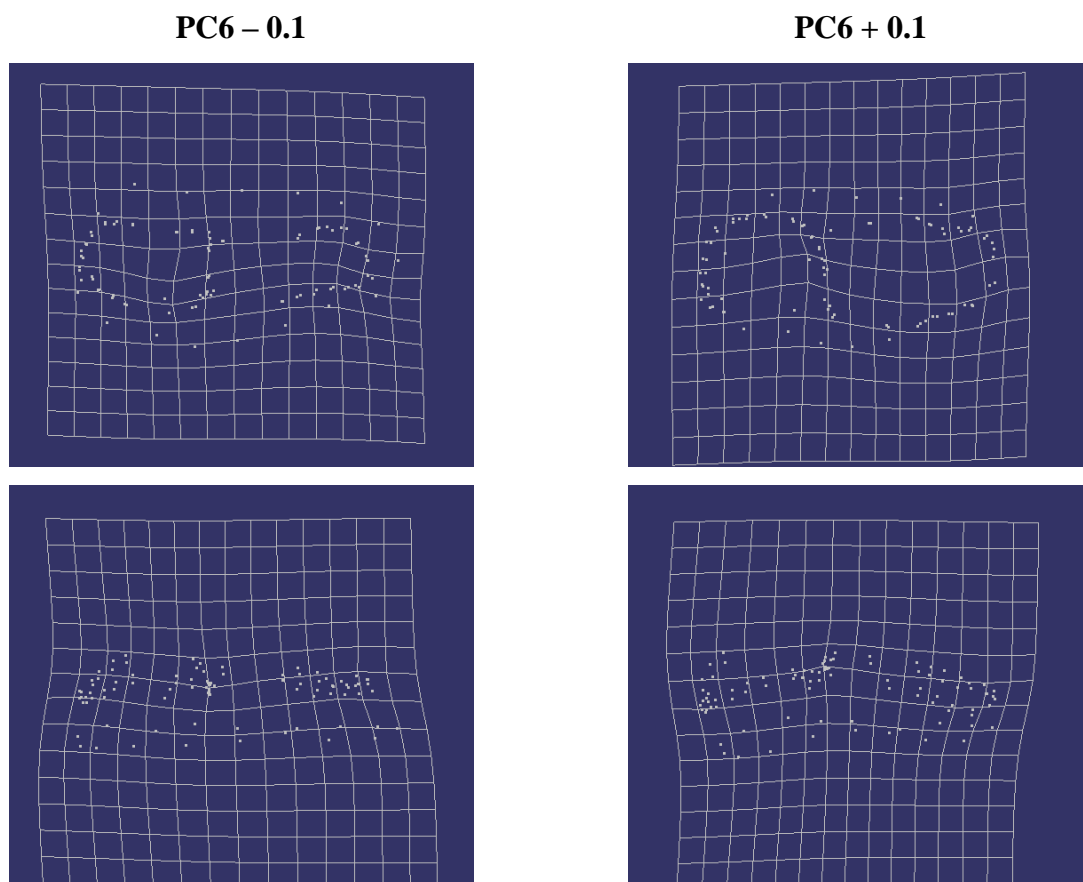


Figure 15 Thin plate spline and location of landmarks in occlusal (first row) and lateral view (second row) along PC6 axis at -0.1 and +0.1, showing the hot-spots of shape change along this axis.

PC7:

The Conturines group shows very little variation along this axis, while the Gamssulzen group has the highest variation (Figure 16). The groups cannot be separated. With more negative values Protocone 1 and 2 are located closer together and the Metastyle becomes taller and moves more centrally (Figure 17). The Metaloph is positioned more mesially, thus reducing the Trigonid.

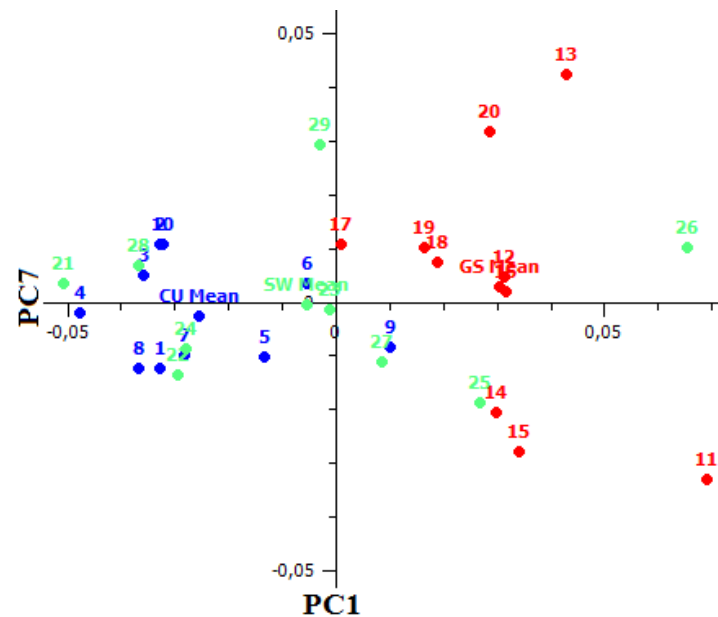


Figure 16 PC1 vs. PC7 in shape space.

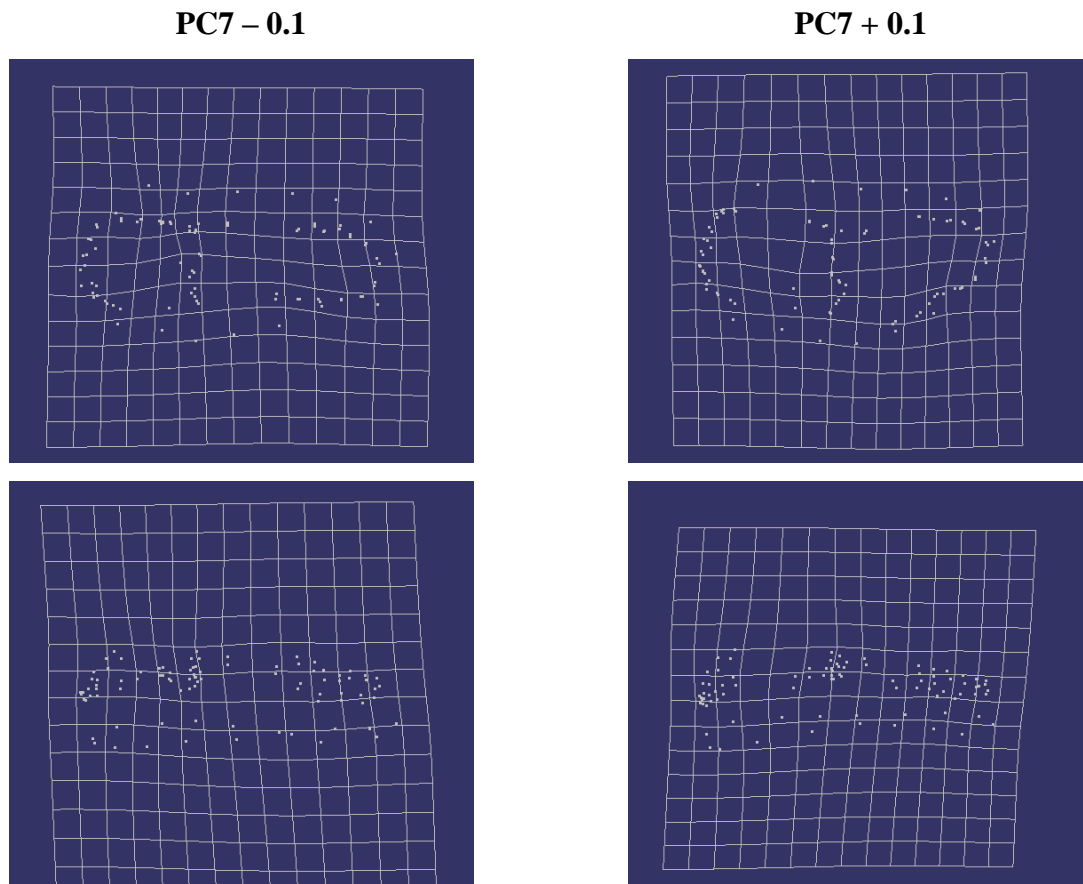


Figure 17 Thin plate spline and location of landmarks in occlusal (first row) and lateral view (second row) along PC7 axis at -0.1 and +0.1, showing the hot-spots of shape change along this axis.

### 3.4) PCA in Form Space

Since there is no significant difference in centroid size between the 3 groups, size does not play an important role on shape differences. Figure 18 shows PC1 and PC2 in form space. As with the centroid size and linear length there is a difference for the means but in form space PC1 does not separate the groups at all. The variation along PC1 is about the same among the three groups. Along PC1 there is a slight change in shape (Figure 19) but it is mostly restricted to slight lateral bending. Specimens with a lower centroid size value show the same tendencies along PC2 as in the shape space PC1 (Figure 20). In short, they are convex both along the median and horizontal planes; and the occlusal surface becomes broader.

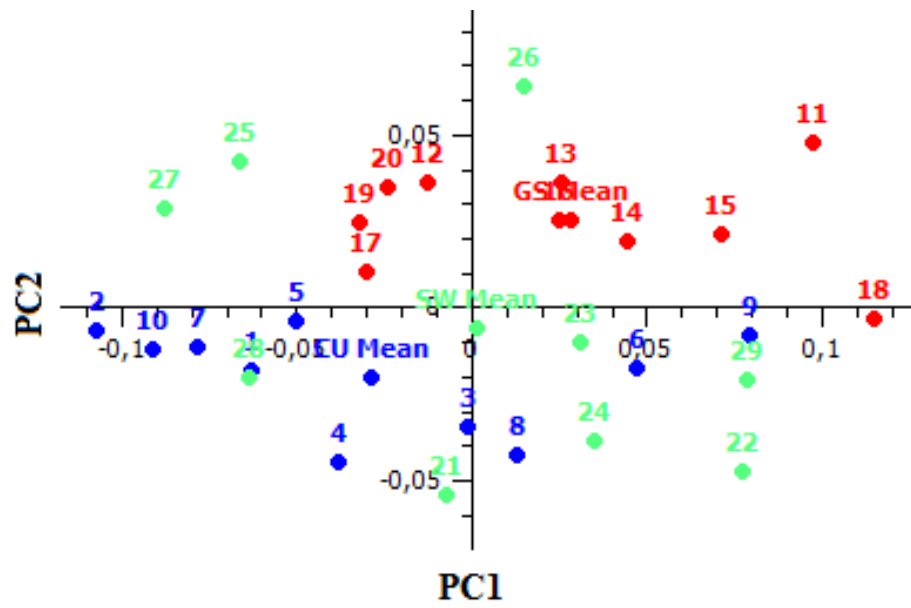


Figure 18 PC1 vs. PC2 in form space.

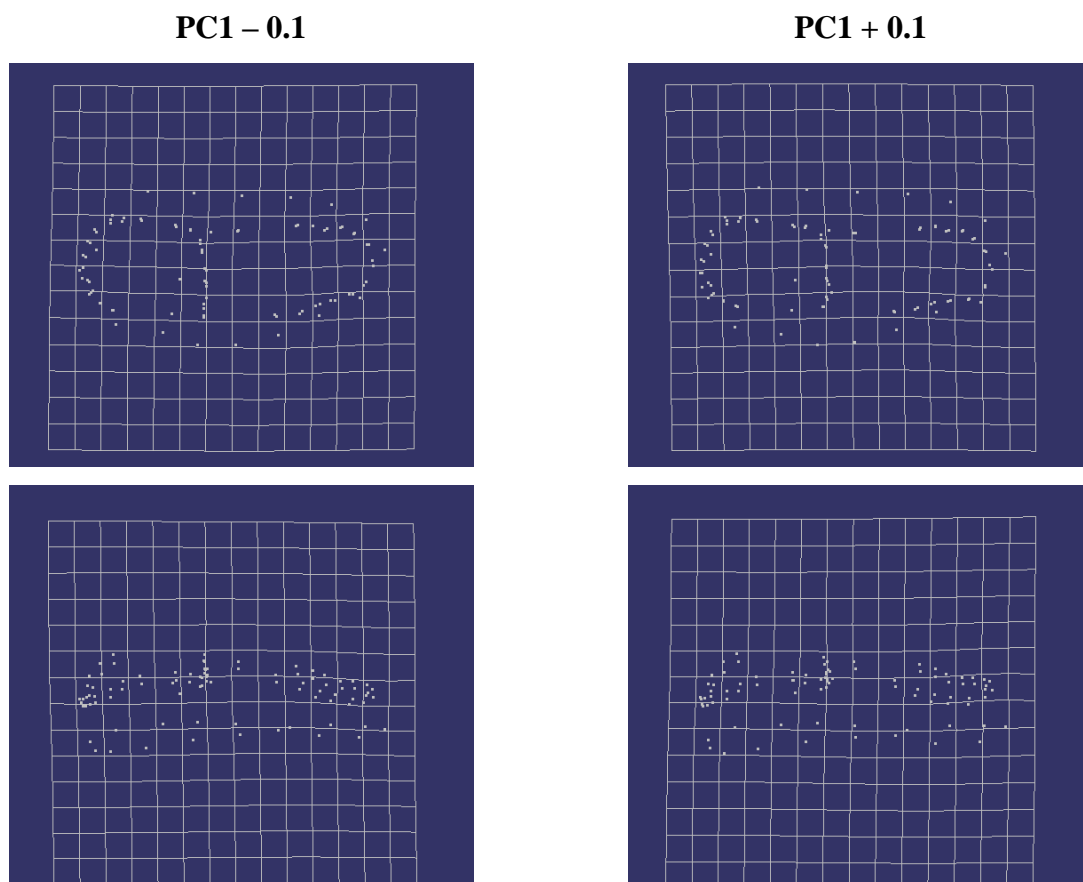


Figure 19 Thin plate spline and location of landmarks in occlusal (first row) and lateral view (second row) along PC1 axis at -0.1 and +0.1 in form space, showing the hot-spots of shape change along this axis.

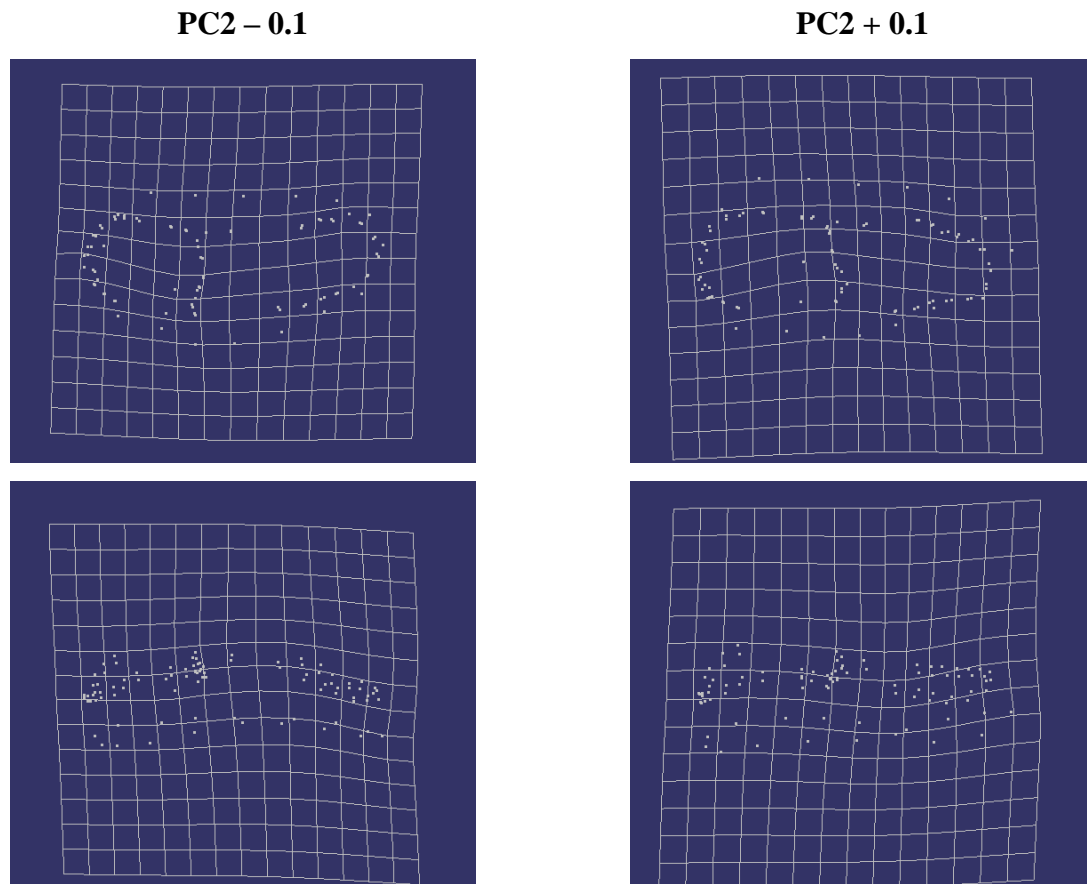


Figure 20 Thin plate spline and location of landmarks in occlusal (first row) and lateral view (second row) along PC2 axis at -0.1 and +0.1 in form space, showing the hot-spots of shape change along this axis.

### 3.5) Allometry

Allometry was only tested for the first seven Principal Components. All show minimal influence of size on shape. Neither in shape space (Table 20) nor in form space (Table 21) are any of the first seven principal components significantly influenced by size. The differences in shape are independent of size.

Shape space PC	RV-Coefficient	p value for F-test	Intercept	Slope
PC1	0.03353	0.17171	0.02559	-10.05815
PC2	0.01789	0.22972	-0.01823	7.16594
PC3	-0.02155	0.52769	-0.00816	3.20754
PC4	0.00355	0.30362	-0.01135	4.46021
PC5	0.06157	0.10363	0.01703	-6.69493
PC6	-0.03574	0.85546	0.00186	-0.73186
PC7	-0.02209	0.53506	-0.00584	2.29513

Table 20 RV coefficient for each PC in shape space regressed on Centroid Size.



Form space PC	RV-Coefficient	p value for F-test	Intercept	Slope
PC1	0.03411	0.16990	-0.02577	10.13229
PC2	0.01771	0.23053	0.01825	-7.17467
PC3	-0.02128	0.52415	0.00825	-3.24416
PC4	0.00388	0.30163	-0.01142	4.49106
PC5	0.06220	0.10249	0.01713	-6.73345
PC6	-0.03572	0.85437	-0.00188	0.73935
PC7	-0.02203	0.53423	0.00587	-2.30671

Table 21 RV coefficient for each PC in form space regressed on Centroid Size.

### 3.6) MANOVA/CVA

Since Centroid size is not significantly different it was not included in the CVA. Instead, the first 10 Principal Component loadings were used.

The CVA based on the first 10 PC scores differentiates very well between the specimens from Conturines cave and Gamssulzen cave (Table 22). All *U. ingressus* from Gamssulzen cave were correctly assigned (100 %), as well as nine out of ten (90 %) *U. ladinicus* from Conturines cave. However, the classification did not succeed well for *U. eremus* from Schwabenreith cave, for which only six out of nine specimens (66%) were classified correctly. Of the total sample in this study, 25 out of 29 specimens (~85 %) have been correctly identified.

	CU	GS	SW	Total # in group
CU	9	0	1	10
GS	0	10	0	10
SW	1	2	6	9
Total classified as	10	12	7	29

Table 22 CVA Confusion matrix based on the first 10 PC scores.

The four specimens that were misclassified are highlighted in Figure 20. In the multi-dimensional space they overlap more than is visible from plotting just the first two Principal Component axes.

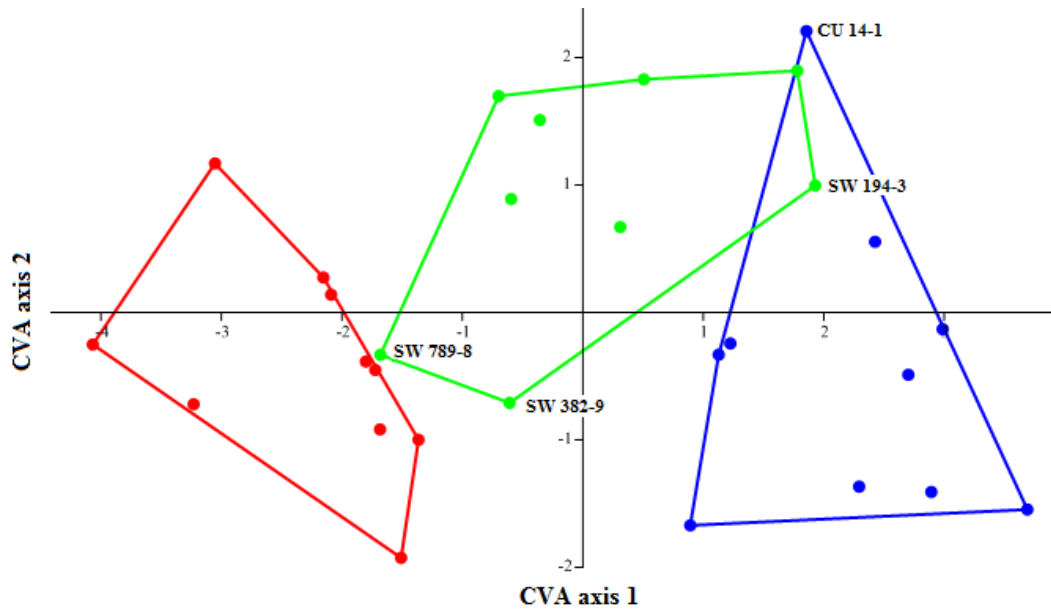


Figure 21 CVA scatter plot (axis 1 vs. 2) based on the first 10 PC scores. The four specimens that were not correctly classified are labeled.

## 4) Discussion

The landmark set used in this study yielded very high results in the classification of individual specimens. Especially *U. ingressus* and *U. ladinicus* were classified correctly in almost 100 % of the cases, using the values of the first 10 PC in a CVA. Since the CVA was not run on the full 28-dimensional dataset but on a reduced 10-dimensional set, there is a possibility that they could be assigned to the correct group, given a larger sample size.

It has previously been established that differences in body size exist among the three species included in this study (Ehrenberg, 1929; Kurten, 1955, Rabeder *et al.*, 2008), as well as body size differences between the sexes (Quiles & Monchot, 2004). However, the test for allometry showed that size is not a good predictor of shape in the studied cave bear sites. These two values are only weakly correlated and the results are not significant. While it cannot be ruled out that some of the other Principal Component values may be more strongly influenced by size, it seems very unlikely. Even if this were the case, any of the untested PC could not account for much of the differences in shape. Since not enough undamaged crania have been found to produce a statistically valid measure of mean size for each species, it is not possible at this point to calculate a  $M^2$  to cranium length ratio.

None of the tested Principal Components show a separation within the groups, underscoring the absence of noticeable differences in relation to sex.

Differences in  $M^2$  tooth shape in this study could not be related to different geographical areas as was suggested by Seetah *et al.* (2012). Had this been the case, the Conturines cave bear would have been less related to the Schwabenreith cave bear. The Gamssulzen and Schwabenreith cave bears do overlap in shape, but less so than the Schwabenreith and Conturines cave bears. Given that *U. eremus* and *U. ingressus* developed in different parts of the Eurasian continent for several hundred thousand years this overlap is surprising and indicates a more similar, albeit not the same, environment, than between *U. eremus* and *U. ladinicus*, which were segregated by elevation. The selective pressures must have been relaxed for the Schwabenreith population, as is obvious from their high degree of variability.

The fact that the teeth from the Conturines and Schwabenreith localities are more alike than they are like those from Gamssulzen could also be due to *U. ladinicus* and *U. eremus* being genetically more closely related to one another than either is to *U. ingressus*, whose ancestors split off from the *Ursus spelaeus* line about 130,000 years ago and who immigrated back into Europe not earlier than 60,000 years ago (Hofreiter, 2005).

Differences in the  $M^2$  shape cannot solely be explained by elevation. However, both the Gamssulzen and Conturines cave bears are much more restricted in the variability of the shape along PC1, while the Schwabenreith bears are much more variable, spanning the entire range of variation, and possibly representing the ancestral condition. This indicates a relaxed restriction on  $M^2$  shape in *U. eremus*. The higher variability could be due to more favorable environmental conditions in lower elevations, i.e. softer food that does not abrade the teeth as much, thus not selecting against cave bears with a wider variety of tooth shapes. The relaxed selective pressure would then not have removed cave bears with less adapted teeth from the population. To test how well they represent the ancestral condition their variability should be compared to  $M^2$  variability in *U. deningeri*, the likely ancestor of cave bears.

Another reason could be the much younger geological age of the specimens from Gamssulzen cave and thus a longer evolutionary time. Given that we don't know the exact selective pressures that shaped *Ursus ingressus*, the differences in shape might also be a result of differences in the habitat which gave rise to this species. Since Conturines is the cave bear site at the highest known elevation to date, and Schwabenreith is located at a lower elevation than

Gamssulzen, it seems unlikely that they encountered the same vegetation. While the relatively small difference in elevation between Gamssulzen and Schwabenreith may not have led to very different vegetation, the fact that the Middle Würmian, during which Gamssulzen cave was utilized was much colder than the Early Würmian (Rabeder *et al.*, 2000), during which cave bears hibernated in Schwabenreith cave supports this argument. The population at Conturines is younger and could possibly only have been successful in populating areas at higher elevation due to an increased adaptation in molar shape.

The groups show much less restriction along the PC2 axis and display about the same amount of variability in shape. It seems surprising that no selection towards a broader talonfield is apparent. Since the broad talonfield is associated with a better ability to shear tough, abrasive foods and mash fruit this would be one of the most obvious features in a herbivore.

## 5) Conclusion

As shown above, differences between the  $M^2$  shapes in cave bears do exist. The highest variability was found in the degree of lateral bending and convexity in the occlusal view. This separated the Gamssulzen cave bears from the other two species, which are genetically more closely related to one another. Using this landmark set on isolated, unworn,  $M^2$  from different sites could potentially allow us to distinguish between the cave bear species at any given locality with high probability. Comparison of shape within the species will be necessary to ensure that not only these three populations can be identified, but the species as a whole.

Differences in shape could not be attributed to different geographic regions but to differences in elevation, with the lowest living population showing the most variation. It was possible to test the most obvious hypothesis, namely that the  $M^2$  from Conturines cave were more laterally bent than those from the other two sites due to their belonging in relatively smaller jaws. The  $M^2$  from Conturines is not only absolutely, but also relatively shorter (Tables 13 & 14) than the others. The overall reduction of body size, which is also visible in the jaw, suggests a colder environment with less available food, to which the Conturines population is adapted. Due to the stronger curvature the shorter mesio-distal length does not necessarily reflect a smaller occlusal surface. Stronger curvature of the  $M^2$  allows for a further reduction of maxilla length while retaining a relatively large surface area. Differences in shape can possibly also be attributed to differences in diet, but this hypothesis needs to be tested further.

The fact that the Schwabenreith and Conturines cave bear molars are more similar in shape could also be due to phylogeny.

## **6) Outlook**

Although the variation for the sample used in this study resembles the variation of the specimens at the respective sites, a larger sample would be needed to achieve better statistical results and to ensure that outliers do not skew the results. In addition more caves need to be sampled to analyze intraspecific variation over time, or due to location, as was suggested by Seetah *et al.* (2012).

To further study the relationship of  $M^2$  shape with overall body size, a larger number of complete maxillae or mandibles are needed to calculate statistically significant mean values of tooth row length spanning from C to  $M^2$ . Additionally, the very small sexual dimorphism could still require that the sexes be analyzed separately due to compounding effects in each tooth. The occlusal surface area, instead of simple mesio-distal linear length, should be measured and compared among the three species to test the hypothesis of a reduction in jaw length while retaining grinding area.

To better test the predictive capabilities of the landmark protocol in a CVA, the sample size needs to be increased to at least double the number that was available for this study ( $n=29$ ).

## **7) Acknowledgements**

I would like to thank Prof. Gernot Rabeder and Prof. Gerhard Weber for supervising and guiding me during this study. I would also like to thank Prof. Fred Bookstein, Cinzia Fornai (Msc.), Dr. Stefano Benazzi, Dr. Michael Coquerelle, Dr. Sascha Senck and Dipl.-Ing. Falk Mazelis for helping me with questions concerning the applied methods. Thanks to Mag. Martin Dockner and Dipl.-Biol. Rica Stephanek for scanning the teeth; Mag.a Christine Frischauf, Mag. Eric Wolfgring and Stefanie Fassl for discussions and helping with the images; Catalina Villamil (M.S.), Elissa Ludeman (M.A.), Rob Thomas and Waldo Mazelis (B.S.) for discussions over coffee and for helping me with the editing of this thesis.

## 8) References

- Bocherens H., Billiou D., Patou-Mathis M., Bonjean D., Otte M., Mariotti A.; 1997; Paleobiological Implications of the Isotopic Signatures  $^{13}\text{C}$ ,  $^{15}\text{N}$  of Fossil Mammal Collagen in Scladina Cave (Sclayn, Belgium). *Quaternary research*, 48(3), 370-380
- Bocherens H., Stiller M., Hobson K., Pacher M., Rabeder G., Burns J., Tütken T., Hofreiter M.; 2011; Niche partitioning between two sympatric genetically distinct cave bears (*Ursus spelaeus* and *Ursus ingressus*) and brown bear (*Ursus arctos*) from Austria: Isotopic evidence from fossil bones; *Quaternary International* 245:238-248
- Bocherens H., Bridault A., Drucker D., Hofreiter M., Münzel S., Stiller M., van der Plicht J.; 2013; The last of its kind? Radiocarbon, ancient DNA and stable isotope evidence from a late cave bear (*Ursus spelaeus* ROSENMÜLLER, 1794) from Rochedane (France). *Quaternary International*
- Bookstein F.; 1991; *Morphometric tools for landmark data: geometry and biology*; Cambridge University Press
- Debeljak I.; 1996; A Simple preparation technique of cave bear teeth for age determination by cementum increments; *Revue de Paleobiologie* 15:105-108
- Döppes D., Rabeder G. (eds.); 1997; *Pliozäne und Pleistozäne Faunen Österreichs*; Verlag der Österreichischen Akademie der Wissenschaften, Wien, pps:411
- Döppes D., Rabeder G., Stiller M.; 2011; Was the middle Würmian in the High Alps warmer than today?; *Quaternary International* 245:193-200
- Ehrenberg K.; 1929; Die Ergebnisse der Ausgrabungen in der Schreiberwandhöhle am Dachstein; *Paläont. Z.*, 11:261–268
- Ehrenberg K.; 1931; Die Variabilität der Backenzähne beim Höhlenbären; In: *Die Drachenhöhle bei Mixnitz* 7-9:535-573, Wien
- Fernández-Mosquera D., Vila-Taboada M., Grandal-d'Anglade A.; 2001; Stable isotopes data ( $\Delta^{13}\text{C}$ ,  $\Delta^{15}\text{N}$ ) from the cave bear (*Ursus spelaeus*): a new approach to its palaeoenvironment and dormancy; *Proc. R. Soc. Lond.* 268:1159-1164
- Fladerer F.; 1992; Erste Grabungsergebnisse von der Schwabenreithhöhle bei Lunz am See (Niederösterreich); *Die Höhle* 43:84-92

Frischauf C., Rabeder G.; in press; The Late Pleistocene immigration of *Ursus ingressus* (Ursidae, Mammalia) in the Alps and the extinction pattern of cave bears; Quaternary International

Germonpré M., Sablin M.; 2001; The cave bear (*Ursus spelaeus*) from Goyet, Belgium. The bear den in Chamber B (bone horizon 4); Bulletin-Institut royal des sciences naturelles de Belgique. Sciences de la terre 71:209-233

Hammer Ø., Harper D., Ryan P.; 2001; PAST: Paleontological Statistics Software Package for Education and Data Analysis; Palaeontologia Electronica 4:9pp

Hille P., Rabeder G. (Eds.); 1986; Die Ramesch-Knochenhöhle im Toten Gebirge, vol. 6. Mitteilungen Quartärkommission der Österreichischen Akademie der Wissenschaften, pp. 1-66

Hofreiter M., Capelli C., Krings M., Waits L., Conard N., Münzel S., Rabeder G., Nagel D., Paunovic M., Jambresic G., Meyer S., Weiss G., Pääbo S.; 2002; Ancient DNA analyses reveal high mitochondrial DNA sequence diversity and parallel morphological evolution of Late Pleistocene cave bears; Molecular Biology and Evolution 19:1244–1250

Hofreiter M., Rabeder G., Jaenicke-Després V., Withalm G., Nagel D., Paunovic M., Jambresic G., Pääbo S.; 2004; Evidence for reproductive isolation between cave bear populations; Current Biology 14:40-43

Hofreiter M.; 2005; Evolutionsgeschichte alpiner Höhlenbären aus molekulargenetischer Sicht; Mitt. Komm. Quartärforsch. Österr. Akad. Wiss.; 14:67–72

Holland L.; 2013; Correlation between the degree of dental abrasion, ontogenetic age and nutrition of Alpine cave bears (DARA method), Diploma thesis, University of Vienna

Kurten B.; 1955; Sex dimorphism and size trends in the cave bear, *Ursus spelaeus* Rosenmüller and Heinroth; Acta Zool. Fennica 90:1-48

Kurten B.; 1976; The cave bear story. Life and death of a vanished animal; New York, Columbia University Press, 163 pp

Loreille O., Orlando L., Patou-Mathis M., Philippe M., Taberlet P., Hänni C.; 2001; Ancient DNA analysis reveals divergence of the cave bear, *Ursus spelaeus*, and brown bear, *Ursus arctos*, lineages; Current Biology 11:200-203

Nagel D.; 2000; Tierische Feinde des Höhlenbären; IN Der Höhlenbär: Herausgegeben und mit einem Vorwort von Wighart v. Koenigswald; Jan Thorbecke Verlag, Stuttgart, pp. 44-47

- Pacher M.; 2000; Taphonomische Untersuchungen der Höhlenbärenfundstellen in der Schwabenreith-Höhle bei Lunz am See (Niederösterreich); Beitr. Paläont. 25:11-85
- Pacher M., Stuart A.; 2008; Extinction chronology and paleobiology of the cave bear (*Ursus spelaeus*); Boreas 38:189-206
- Peigné S., Goillot C., Germonpré M., Blondel C., Bignon O., Merceron G.; 2009; Predormancy omnivory in European cave bears evidenced by a dental microwear analysis of *Ursus spelaeus* from Goyet, Belgium; PNAS 106:15390-15393
- Quiles J., Monchot H.; 2004; Sex ratio and mixture analysis of *Ursus spelaeus* (Carnivora, Ursidae) from the Upper Pleistocene site of Fate (Liguria, Italy). The palaeobiological implications; Annales de Paléontologie 90:115–133
- Rabeder G., Steffan I., Wild E.; 1994; The chronological position of the cave bears from Conturines cave; Abstract 2<sup>nd</sup> Int. cave bear symposium Alta Badia
- Rabeder G. (ed.); 1995; Die Gamssulzenhöhle im Toten Gebirge - Mitteilungen der Kommission für Quartärforschung der Österreichischen Akademie der Wissenschaften 9, 1-133, Wien
- Rabeder G.; 1999; Die evolution des Höhlenbärengebisses (Vol. 11); Verlag d. Österr. Akad. d. Wiss.
- Rabeder G., Pacher M., Nagel D.; 2000; Der Höhlenbär: Herausgegeben und mit einem Vorwort von Wighart v. Koenigswald; Jan Thorbecke Verlag, Stuttgart
- Rabeder G., 2001. Geschlechtsdimorphismus und Körpergröße bei hochalpinen Höhlenbärenfaunen; Beitr. Palaont., 26:117–132, Wien
- Rabeder G., Hofreiter M., Nagel D., Withalm G.; 2004; New taxa of alpine cave bears (Ursidae, Carnivora); Cahiers scientifiques-Muséum d'histoire naturelle de Lyon; 49-67
- Rabeder G., Hofreiter M.; 2004; Der neue Stammbaum der alpinen Höhlenbären; Die Höhle 55:1-19
- Rabeder G., Frischauf C., Withalm G.; 2006a; La grotta delle Conturines e l'orso ladinico – Conturines Cave and the Ladinic Bear – Die Conturineshöhle und der Ladinische Bär; Consorzio Turistico Alta badia 34pp, Corvara
- Rabeder G., Tsoukala E., Kavcik N; 2006b; Chronological and systematic position of cave bears from Loutrá Aridéas (Pella, Macedonia, Greece); Scientific Annals, School of Geology Aristotle University of Thessaloniki (AUTH) 98:69-73



Rabeder G.; 2007; Evolution, Migration und Klimageschichte in den Alpen am Beispiel der Bären (Ursidae, Mammalia); *Denisia* 20:745-752

Rabeder G., Debeljak I., Hofreiter M., Withalm G.; 2008; Morphological responses of cave bears (*Ursus spelaeus* group) to high-alpine habitats; *Die Höhle* 1-4:59-72

Rosendahl W.; Döppes D.; 2006; Trace fossils from bears in caves of Germany and Austria; *Scientific Annals, School of Geology Aristotle University of Thessaloniki (AUTH)* 98:241-249

Rabeder G., Withalm G.; 2011; On the Peculiarities of the Cave Bears from Ajdovska jama near Krško (Slovenia); *Mitt. Komm. Quartarforsch. Osterr. Akad. Wiss.*, 20:73–78, Wien

Richards M., Pacher M., Stiller M., Quiles J., Hofreiter M., Constantin S., Zilhao J., Trinkhaus E.; 2008; Isotopic evidence for omnivory among European cave bears: Late Pleistocene *Ursus spelaeus* from the Pesteră cu Oase, Romania; *PNAS* 105:600-604

Robert P., Escoufier Y.; 1976; A Unifying Tool for Linear Multivariate Statistical Methods: The RV-Coefficient; *Appl. Statist.* 25:257-265

Rohlf J., Corti M.; 2000; Use of two-block Partial Least-Squares to study covariation in shape; *Syst. Biol.* 49:740-753

Seetah K., Cardini A., Miracle P.; 2012; Can morphospace shed light on cave bear spatial-temporal variation? Population dynamics of *Ursus spelaeus* from Romualdova pecine and Vindija, (Croatia); *Journal of Archaeological Science* 39:500-510

Spoor F., Zonneveld F., Macho G.; 1993; Linear measurements of cortical bone and dental enamel by computed tomography: applications and problems; *American Journal of Physical Anthropology* 91(4):469-484

Temmel H.; 1996; Die Mittelpleistozänen Bären (Ursidae, Mammalia) aus der Schachtfüllung der Repolusthöhle bei Peggau in der Steiermark; *Dissertation Universität Wien*

Torres T., Ortiz J., Cobo R., de Hoz P., Garcia-Redondo A., Grün R.; 2007; Hominid exploitation of the environment and cave bear populations. The case of *Ursus spelaeus* Rosenmüller-Heinroth in Amutxate cave (Aralar, Navarra-Spain); *Journal of Human Evolution* 52:1-15

Vila Taboada M., Fernandez Mosquera D., Grandal d'Anglade A.; 2001; Cave bear's diet: a new hypothesis based on stable isotopes; *Cadernos Lab. Xeoloxico de Laxe* 26:431-439

Weber G., Bookstein F.; 2011; *Virtual Anthropology: A guide to a new interdisciplinary field*; Springer

Withalm G.; 2008; Harris-Linien beim Höhlenbären – ein interessanter methodischer Ansatz in der Paläobiologie; Speldok 18:49-64

Withalm G.; 2001; Die Evolution der Metapodien in der Höhlenbären-Gruppe (Ursidae, Mammalia); Dissertation, Universität Wien

## 9) Abstract

In this study the upper 2<sup>nd</sup> molars from three alpine cave bear sites (Conturines cave, Gamssulzen cave and Schwabenreith cave) were analyzed using 3D geometric morphometrics. Each of these caves was used as place to hibernate by a different species of cave bears, *Ursus ladinicus*, *U. ingressus* and *U. eremus*, respectively. The analysis was based on a set of 18 landmarks and seven curves with 71 semi-landmarks, placed on a 3D model which was created from CT-scans.

A Canonical Variance Analysis based on the first 10 Principal Component values for each specimen was able to separate the three groups with high accuracy (~85 %). The main shape variables include bucco-lateral bending, occlusal bending and a broadened talonfield. Shape differences are unlikely to be the result of different geographical regions but seem to be associated with the elevation of the caves and the species they belong to. The observed curving of the M<sup>2</sup> is likely a result of two counteracting forces: Size constraint due to reduced availability of food and necessity to reduce body size as well as the need to retain a large grinding surface for the processing of tough foods.

## 10) Zusammenfassung

Für diese Arbeit wurde der zweite obere Molar aus drei alpinen Höhlen (Conturines, Gamssulzen und Schwabenreith) mittels 3D Geometric Morphometrics analysiert. Jede dieser Höhlen wurde von einer anderen Höhlenbärenart (*Ursus ladinicus*, *U. ingressus* und *U. eremus*) zum Winterschlaf aufgesucht. Die Analyse basiert auf einem Landmarkset aus 18 Landmarks, so wie sieben Kurven mit insgesamt 71 Semi-Landmarks. Die Landmarks und Kurven wurden auf 3D Modellen plziert welche aus CT-Scans erstellt wurden.

Eine Canonical Variance Analysis, basierend auf den Werten der ersten 10 Hauptkomponenten jedes Elements, konnte die drei Gruppen mit hoher Genauigkeit (~85%) unterteilen. Entlang der ersten zwei Hauptkomponenten Achsen sind die grössten Unterschiede in der Gestalt der Zähne eine bucco-laterale, so wie eine occlusale Krümmung und eine Verbreiterung des Talonfeldes. Die Unterschiede in der Gestalt konnten nicht auf die geographische Lage zurückgeführt werden. Sie sind wahrscheinlicher mit der Lage der Höhle ueber der Seehöhe und den dort herrschenden klimatischen Bedingungen verbunden. Phylogenetische Einflüsse sind auch nicht auszuschliessen. Die festgestellte Krümmung des  $M^2$  ist vermutlich ein Resultat von zwei gegensätzlich wirkenden Kräften: Eine Reduktion der Körpergrösse aufgrund von selteneren Nahrungsvorkommen so wie die Notwendigkeit einer möglichst grossen Kaufläche auf den Molaren um robustere/zähere Nahrung zermahlen zu koennen.

## 11) Appendix

Specimen	Scan Resolution (micron)	Scanner	Date	Max. Length (mm)	Max. Width (mm)
SW_1032-4	45	Anthropology	May 2012	39.65	20.12
SW_1706	44.18	Paleontology	July 2012	40.80	21.00
SW_1869	46.32	Paleontology	July 2012	46.20	23.20
SW_194-3	44.89	Paleontology	July 2012	42.87	20.99
SW_220-3	45	Anthropology	June 2012	40.66	22.4
SW_359-1	35	Anthropology	May 2012	46.10	24.20
SW_382-9	45	Anthropology	May 2012	43.13	22.57
SW_468-5	47	Anthropology	July 2012	43.40	21.70
SW_789-8	44.89	Paleontology	July 2012	40.65	19.81
SW_882	49.88	Paleontology	June 2012	42.50	22.70
CU_1-2	45	Anthropology	July 2012	39.18	19.56
CU_14-1	35	Anthropology	Feb. 2012	41.04	21.82
CU_21-2	35	Anthropology	Feb. 2012	40.65	19.44
CU_29-2	45	Anthropology	July 2012	43.43	23.06
CU_29-4	45	Anthropology	June 2012	41.96	21.50
CU_31-1	42.04	Paleontology	May 2012	38.42	19.84
CU_38-2	44.89	Paleontology	July 2012	38.27	20.06
CU_4-1	42.75	Paleontology	June 2012	38.15	19.25
CU_53-2	47	Anthropology	July 2012	42.42	21.57
CU_55-1	44.89	Paleontology	June 2012	44.45	22.74
CU_6	45	Anthropology	May 2012	41.30	21.40
GS_109-1	47.74	Paleontology	June 2012	47.73	24.08
GS_12-3	44.89	Paleontology	June 2012	46.56	24.05
GS_147-3	44.89	Paleontology	July 2012	43.28	20.43
GS_148-1	45	Anthropology	July 2012	41.41	20.90
GS_157-1	47	Anthropology	July 2012	47.69	26.04
GS_194-2	42.04	Paleontology	May 2012	41.70	21.16
GS_197-1	47.03	Paleontology	June 2012	40.87	21.76
GS_202-1	45	Anthropology	June 2012	43.57	22.29
GS_26-3	44.89	Paleontology	June 2012	40.96	22.23
GS_27-1	44.89	Paleontology	July 2012	43.88	22.15
GS_38-1	45	Anthropology	May 2012	42.19	22.65

Table 23 Complete list of all specimens in this study. Anthropology = Dept. of Anthropology, Univ. of Vienna.  
Paleontology = Dept. of Paleontology, Univ. of Vienna

<b>Specimen #</b>	<b>Side</b>	<b>Sex</b>	<b>Length in mm</b>
CU 720	dex	m	104.7
CU 716	sin	m	96.2
CU 863	dex	f	89.5
CU 695	dex	m	97.8
CU 12	dex	f	95.4
CU 501-1	dex	f	96.1
CU 501-2	dex	m	104.8
CU 670	sin	m	100.4
GS 150-2	sin	f	92.3
GS 150-3	dex	f	93.9
GS 150-5	dex	m	100.6
GS 753-3	dex	m	99.8
GS 45-7	sin	f	94.6
GS 29-1	dex	m	105.9
GS 41-2	dex	f	98.8
GS 455-2	dex	f	99.2
GS 512-2	sin	f	93.3
GS 718	dex	m	103.9
GS 697	dex	m	105
GS 512-1	dex	f	99.3
GS 714-2	dex	m	104.8
GS 46-1	dex	f	98
GS 2-27	dex	m	108.9
GS 718	sin	m	104.6
GS 513	dex	m	101.8
GS 714-1	sin	u	105.6
GS 33-15	dex	f	94.6
GS 26-189	sin	m	97.3
GS 26-188	sin	f	99.4
GS 171-1	dex	m	104.1
SW 1628	dex	f	92.5
SW 362	dex	m	105.3
SW 1244	dex	f	98.6
no no.	sin	f	98.7
SW 140	sin	f	94.4
SW 156	sin	m	105.9
SW 1002	dex	m	101.5
SW 1328	sin	m	107.4
SW 795	sin	f	102.4
SW 225	sin	f	94.5
SW 583	sin	f	96.8
SW 438	sin	f	91.5
SW 1229	dex	f	103.4
SW 29	dex	f	95.8
SW 566	dex	f	100
SW 379	dex	m	97.8
SW 898	dex	f	96.4
SW 601	sin	f	93.8
SW 1630	sin	m	100.2
SW 593	sin	f	93.7

Table 24 Measurements of mandibular tooth rows p4 - m3 from the three sites used in this study. f = female; m = male.

# 12) Curriculum Vitae

**Eric John Mazelis**

Email: ericmazelis@gmail.com

## EDUCATION

- City University of New York (CUNY), NYC, USA** 09/2012 – ongoing  
PhD studies in evolutionary primatology and physical anthropology as part of the New York Consortium in Evolutionary Primatology (NYCEP)
- University of Vienna, Austria** 10/2007 – 11/2013  
Individual diploma studies (equivalent to Master's degree in the US/UK university system) in Quaternary biology and archaeology of the Paleolithic
- University of Vienna, Austria** 10/2005 – 03/2009  
Diploma studies in Biology
- Elsa-Brändström-Schule (High School), Hannover, Germany** 1999 – 2005  
General qualification for university studies (Abitur)

## WORK EXPERIENCE

- Freelancer for TERRA Environment Engineering, Vienna, Austria** 05/2010 – 04/2012  
*Assistant on various environmental projects*
- Austrian Academy of Science, Vienna, Austria** 03/2011 – 10/2011  
*Laboratory assistant for the preparation of material from past excavations*
- University of Natural Resources and Applied Life Sciences, Institute for applied Geology, Vienna, Austria** 07/2009 – 10/2011  
*Laboratory assistant to Dr. Johanna Lomax at the OSL laboratory*
- Max Planck Institute for Evolutionary Anthropology, Leipzig, Germany** 02/2010  
*Intern at the Department of Human Evolution for four weeks*
- University of Vienna, Department of Paleontology, Austria** 10/2009 – 01/2010  
*Tutor for laboratory course on preparation techniques*
- Museum of Natural History, Stockholm, Sweden** 08/2009 – 09/2009  
*Internship with Dr. Daniela Kalthoff, working on Dentin from *Xenarthra**
- Austrian Academy of Science, Vienna, Austria** 09/2008 – 12/2008  
*Assistant to prepare cave bear bones*
- Mano River Resources Inc., Monrovia, Liberia** 02/2007  
*Assistant at geologic expedition to the Putu mountain range*

## EXCAVATIONS

- Paleontological excavation, Arzberg, Austria** 07/2011 and 07/2012  
*Excavation of cave bears (*Ursus spelaeus*) in the Hochschwab mountain range in the Northern Alps*
- Exploratory Paleontological cave excavation, Pendling, Austria** 06/2011  
*Exploratory excavation to determine the if cave bears (*Ursus spelaeus*) could be found in a cave in the Brandenberger Alps, a subsection of the Northern Alps*
- Paleontological excavation, Kryopigi, Chalkidiki, Greece** 09/2010  
*Excavation of an Upper Miocene hyena den*

<b>Paleontological cave excavation, Vazec, Slovakia</b> <i>Excavation of cave bears (Ursus spelaeus) in the Low Tatras mountain range in central Slovakia</i>	09/2010
<b>Paleolithic excavation, Breitenbach, Germany</b> <i>Excavation of an Aurignacien open air site</i>	08/2010
<b>Paleontological cave excavation, Torstein, Austria</b> <i>Excavation of cave bears (Ursus spelaeus) in the Dachstein Mountain range of the Northern Alps</i>	07/2010
<b>Paleontological cave excavation, Slovakia</b> <i>Excavation of cave bears (Ursus spelaeus) in the Carpathian Mountains in eastern Slovakia</i>	09/2008 and 09/2009
<b>Paleontological excavation of Cretaceous dinosaur footprints, Münchehagen, Germany</b> <i>Excavation of four sets of footprints in sandstone</i>	09/2009
<b>Paleolithic excavation, Krems-Wachtberg, Austria</b> <i>Paleolithic excavation of a 27,000 year old Gravettian open air settlement</i>	07/2009
<b>Paleontological open air site excavation, Bruckneudorf, Austria</b> <i>Excavation of auditory ossicles from Miocene dolphins</i>	08/2008
<b>Paleontological excavation, Teiritzberg, Austria</b> <i>Excavation by the Museum of Natural History, Vienna, to uncover a large Miocene oyster reef for a museum</i>	06/2008